Sample 34 at the waste dumpsite (old) and sample 36 at the town concentrator shows relatively high in water-soluble and ion exchangeable phase. This suggests possibility of an input of concentrator waste.

Sediment samples at the dredging pond PS-5 shows approximately 40% in the sorbed & organic phase and Fe and Mn oxide phase, and approximately 60% in the sulfide phase. The composition is different from other soil samples. Concentration of these phases was also high at over several hundreds of mg/kg. The following table shows the comparison of the average composition and concentration of the pond sediments and auger soil samples. It is considered that concentrator waste was dumped into the dredging pond.

Table 4.1 Comparison of the pond sediment and soil

Sample	Water soluble As (mg/kg)	Ion exchangeable As (mg/kg)	Sorbed & organic As (mg/kg)	Sulfide As(mg/kg)	Fe and Mn oxide As (mg/kg)
Sediment of the dredging pond (average)	13.4	0.92	235	273	77.7
Auger soil (30 cm depth) (average)	1.1	1.7	21	8.4	3.9
Auger soil (100 cm depth) (average)	1.0	1.3	16	9.9	3.9

Sample 39 from the waste dumpsite (new) shows 72% of arsenic is in the sorbed and organic phase while the remain is in the sulfide phase. Sample T-6 from the site 32C, sorbed and organic phase, and Fe and Mn oxide phase reaches 90% of the arsenic.

Sample 2 from the site 32L has composition similar to the average soil but at a concentration over 10 times higher. Nearby sample 31 shows a very high arsenic of 1,600 mg/kg in the sulfide phase. The composition varied significantly. This suggests input of some sort of mining waste.

4.2 Oxidation - Reduction potential (ORP) and arsenic release mechanism

Release of arsenic from Fe oxide or hydroxide was controlled by the oxidation-reduction potential. Fe(II) ion co-precipitates with arsenic in water in the oxidizing condition and forms hydroxide. Fe oxide and hydroxide also adsorbs arsenic very well in the oxidizing condition. However arsenic co-precipitated with Fe, and arsenic adsorbed onto Fe oxide will be released into the environment with the Fe(II) ion under the reducing condition. On the other hand, the possibility of arsenic release from sulfide

is considered small because arsenopyrite is relatively stable under normal conditions.

Fig. 4.8 shows correlation of arsenic and sulfate ion in auger water and in soil elution test. This survey originally assumed arsenopyrite in sediment as one of the potential sources of arsenic. If arsenopyrite is oxidized to release arsenic, it will also release sulfate and iron. Iron was also released not only by oxidation of arsenopyrite but also by reduction of Fe oxide and hydroxide, thus it is not suitable as an indication of arsenopyrite oxidation. From this viewpoint, Fig. 4.8 does not show any correlation between arsenic and sulfate. Therefore it can be concluded that the oxidation of arsenopyrite is not a major pollution contributor in the area.

Fig. 4.9 shows relation between oxidation-reduction potential (ORP) and arsenic content in auger water sampled from the three areas during detailed investigation, namely, around the town concentrator, around the site 32C, and around the site 32L. Samples from site 32C area were gathered in a small area suggesting a single mechanism of arsenic release related to ORP. On the other hand, samples from the town concentrator, and the site 32L were scattered. This implies there is no relation between ORP and arsenic release.

Fig. 4.10 shows ORP-pH diagram by similar grouping. Size of symbols is proportional to arsenic content of auger water. Therefore, larger the symbol, higher the arsenic content. According to the figure, samples at the site 32C are high in arsenic if ORP is more reducing. Samples from the town concentrator have little correlation between ORP and arsenic content. Samples from the site 32L are somewhat in the middle. This suggests high arsenic at the site 32C be related to release from Fe oxide under a reducing condition.

Soil sample T-6-2 from the trench at site 32C during the detailed investigation phase shows that the combined composition of sorbed and organic phase, and Fe and Mn oxide phase reaches 90%. Further the combined concentration is 120 mg/kg. Under reducing condition, if such arsenic is released into pore water, it will form high concentration of arsenic pollution. In fact, high arsenic content and low ORP is well correlated in the samples at the site 32C. Sample 39 from the waste dumpsite (new) also shows that the combined composition of sorbed and organic phase, and Fe and Mn oxide phase reaches 99% and low ORP. This suggests the possibility of same mechanism as the site 32C.

Samples 2-4 and 31-4 at the site 32L show a relatively high composition of sorbed and organic phase, and Fe and Mn oxide phase, but also high in water soluble arsenic at over 10 mg/l. Sample 31-4 shows 66% of the arsenic in sulfide. Therefore, it is estimated that arsenic pollution at the site 32L is partly caused by release from Fe oxide under a

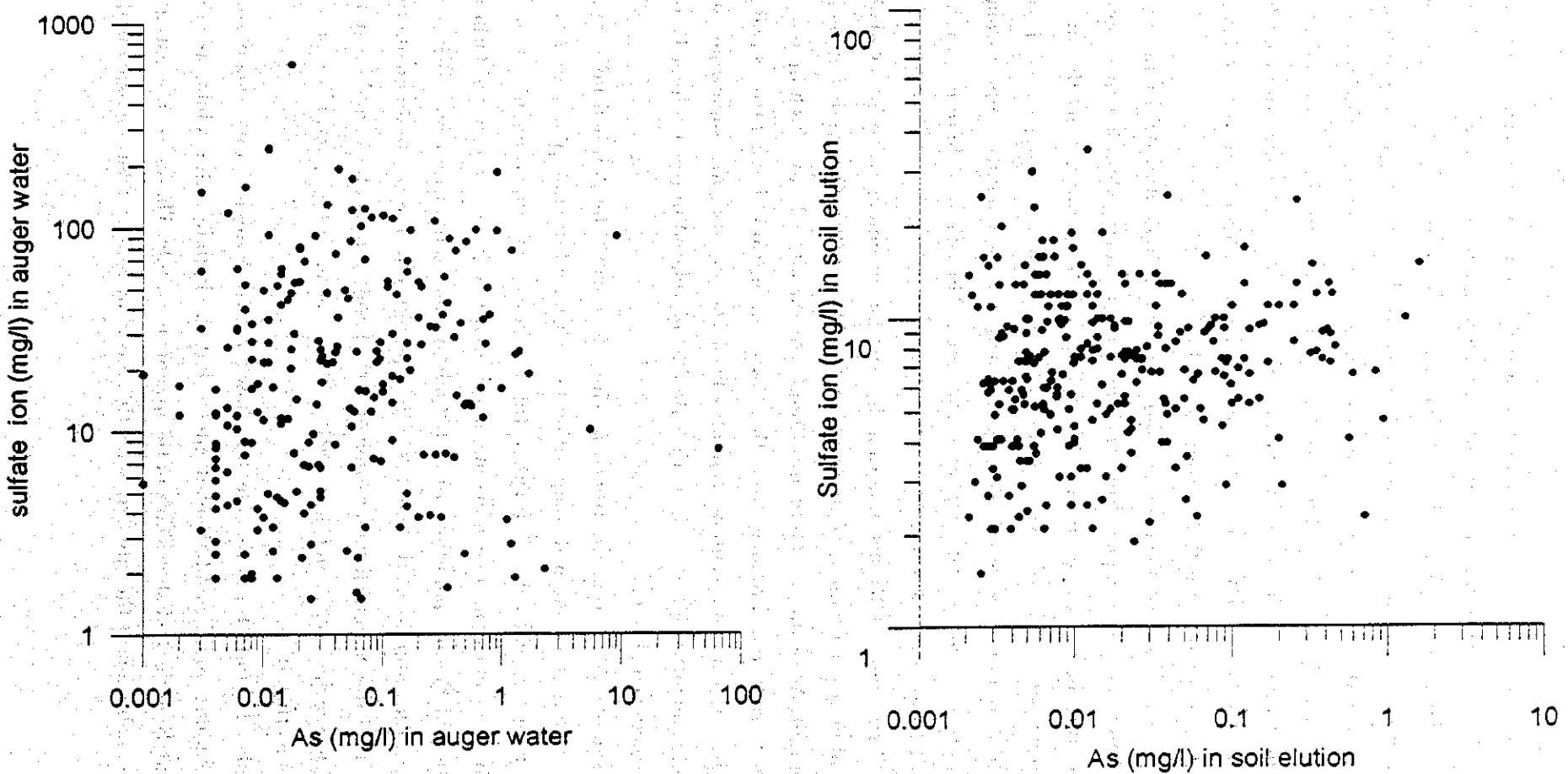

Fig 4.8 Correlation of Arsenic and Suiphate

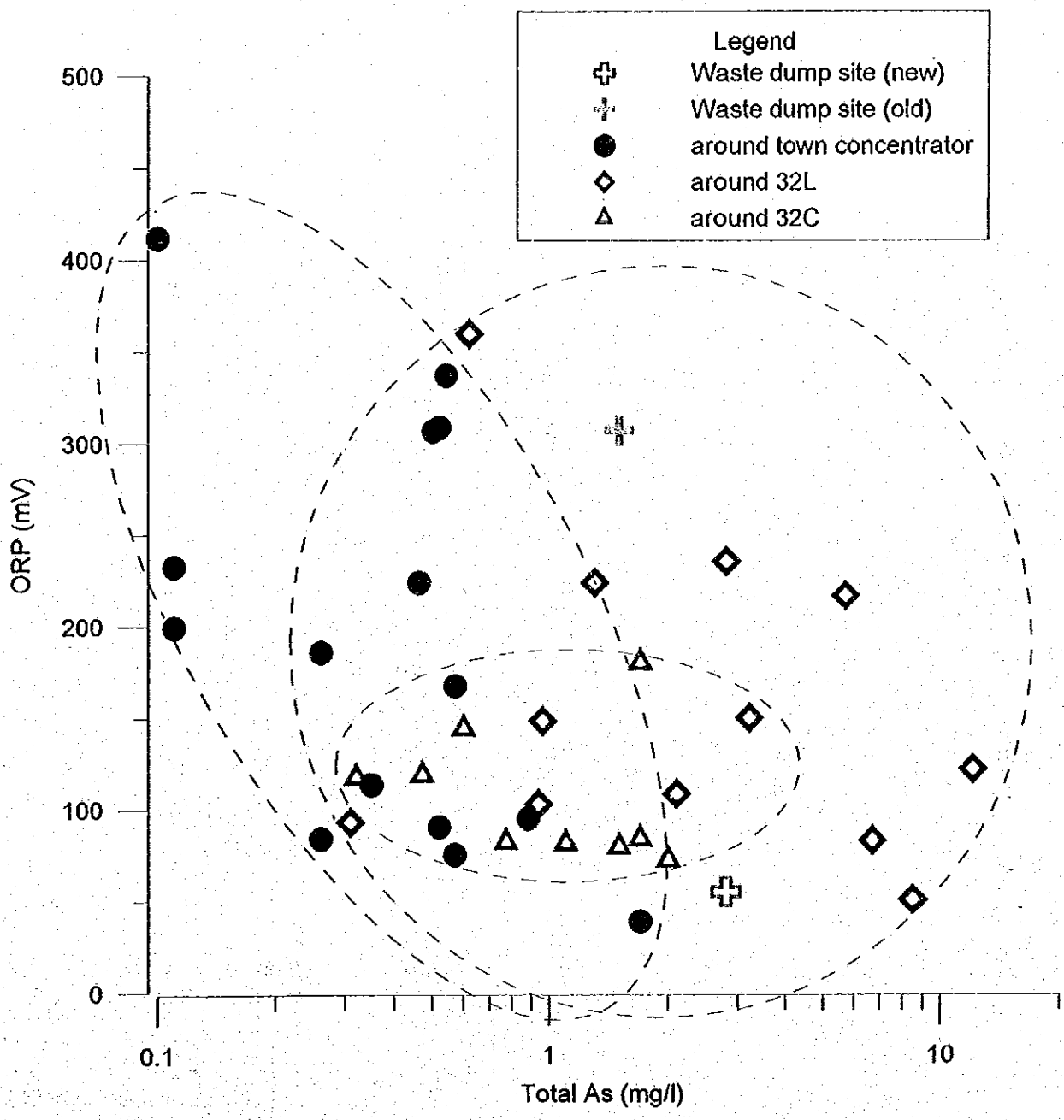

Fig 4.9 Classification of Source by Arsenic and ORP

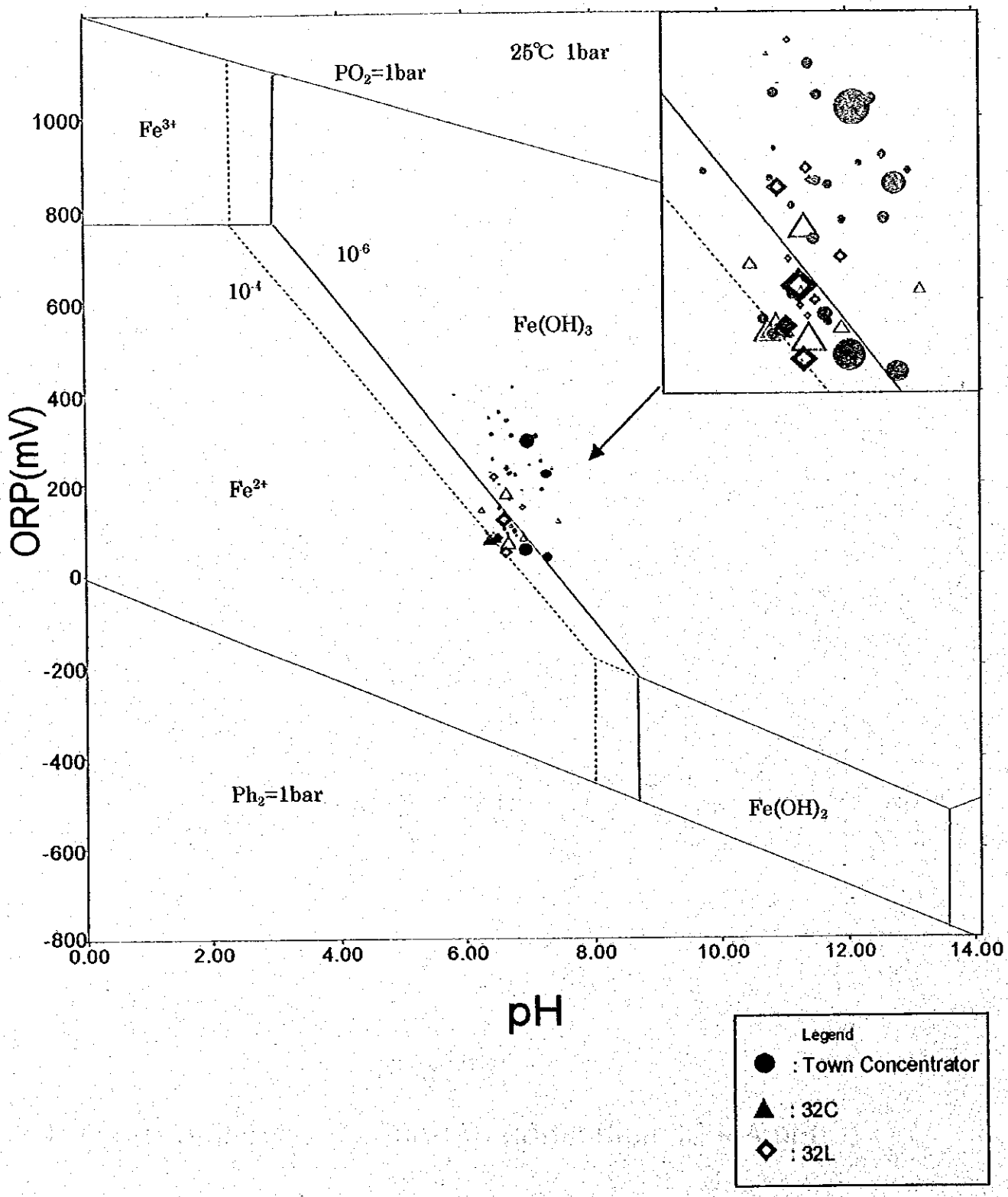

Fig 4.10 ORP-pH Diagram for Fe Hydrooxide

reducing condition, but also caused by simple elution and oxidation of sulfide.

Sample 34 at the waste dumpsite (old) and sample 34 at the town concentrator show fairly high in water soluble phase and low in ORP. A similar mechanism is considered for these sites (Fig. 4.4).

During the detailed investigation, dissolved iron (Fe(II)) was measured in the field using a portable kit (pack test). This was done to check if Fe(II) ion was released from Fe oxide and hydroxide with the arsenic under a reducing condition. As a result, for site 32C, a sample with high arsenic also show a high concentration of Fe(II) ions and low ORP. This confirms the above-discussed mechanism of arsenic releases (Fig. 3.19). Sample 39 at waste dumpsite (new) also shows a high concentration of high Fe(II) ions (Fig. 3.16). Regarding the samples around the town concentrator and the site 32L, some points correlate with high arsenic and Fe(II), but in general there is no significant correlation. Around the site 26M, a high concentration of Fe(II) ions was detected near the pig farm. This indicates a reducing condition caused by organic waste made of Fe oxide to release arsenic and Fe(II) (Fig. 3.23). As discussed, the measurement of Fe(II) ions confirmed that the arsenic release mechanism is under a reducing condition.

4.3 Arsenic species analysis and behavior

Arsenic is the element whose toxicity is changed by its chemical speciation. There is over several hundreds to thousands differences in toxicity between inorganic arsenic in water and organic arsenic in an aquatic organism. Even within inorganic arsenic, trivalent arsenic - As(III) and pentavalent arsenic - As(V) has several times difference in toxicity. As(III) is more toxic than As(V). Furthermore, behavior in soil and groundwater changes by its speciation. As(III) is near neutral in terms of its electric charge and hardly adsorbed, while As(V) is positively charged and easily adsorbed. Therefore, arsenic speciation is important in study of arsenic pollution. In this survey, ion chromatograph-atomic adsorption spectroscopy was installed in the field laboratory and arsenic speciation was analyzed.

Average arsenic speciation in ground water and surface water samples from the detailed investigation is summarized in the following table. As(V) dominates in surface water and approximately 80% of the arsenic is in the form of As(V). For well water, 70% of the arsenic is As(V). On the contrary for auger water freshly sampled (new), 98% is As(III). Auger water sampled one year after being drilled still showed approximately 95% of arsenic in As(III). This can be explained by the oxygen availability. It is largest in river water, while smallest in auger water. Well water has good oxygen contact in case of an open dug well. Auger water sampled one year after

drilling showed a slight increase of As(V), but the change is fairly small.

Table 4.2 As(III) and As(V) distribution

	As(III) mg/l	As(V) mg/l	As(V)/As(III)	ORP(mV)
River water N=34	0.035	0.125	3.578	340
Auger water (new) Measured after drilled. N=29	1.706	0.043	0.025	176
Auger water (old) Measured after one year N=23	1.005	0.060	0.060	261
Well water N=22	0.125	0.344	2.746	325

N= number of samples

A high correlation was noted between the ratio of As(V)/As(III) (converted to logarithm) and ORP (Fig. 4.11) for the average of the group. However, if the same plot was made for individual samples. the correlation is not clear as shown in Fig. 4.12. This may be due to the slow change of arsenic speciation by ORP.

In summary, As(V) dominates in water having long-term contact with the atmosphere, while As(III) dominates in groundwater even at a few meters depth. It is risky to judge the ratio of As(III) and As(V) only from the measurement of ORP. It is suggested that groundwater to be exposed to air long enough, if it is for drinking purpose.

Fig.4.13 shows variation of arsenic species in water of the upstream Huai Ron Na River. Location of the sampling point is shown on the map at the upper left of the figure. The black line indicates total arsenic. red dotted line for As(III). blue dotted line for As(V) and green line for ORP. In general. river water is rich in As(V) as discussed before. However. As(III) increases over As(V) after the point 20 downward. At the same time. total arsenic increases more than 50%. An interesting observation is that Fe oxide was widely distributed in the river sediment at this interval with lower ORP. To explain these phenomena. it is necessary to assume that groundwater rich in As(III) (also rich in Fe(II) ion) flows into the river at this interval. This explanation is in agreement with the distribution of arsenic in auger water of the reconnaissance survey (as shown in the map at upper left). This also indicates that Fe(II) ions flows into the river from groundwater. immediately is oxidized to Fe oxide and precipitates. Conversely. As(III) does not change immediately to As(V) and flows downstream. This is an important

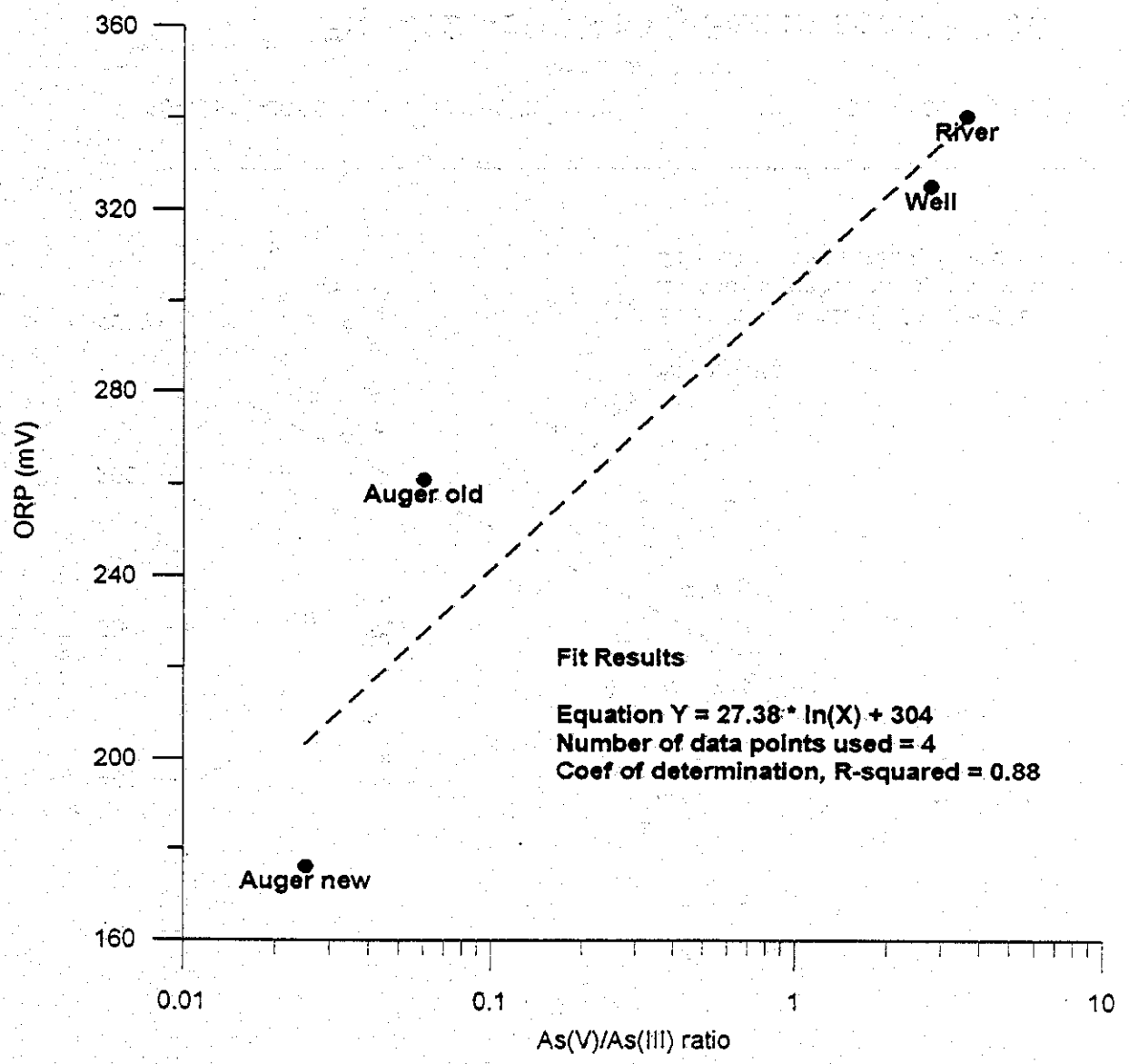

Fig 4.11 As(V)/As(III) Ration and ORP (1)

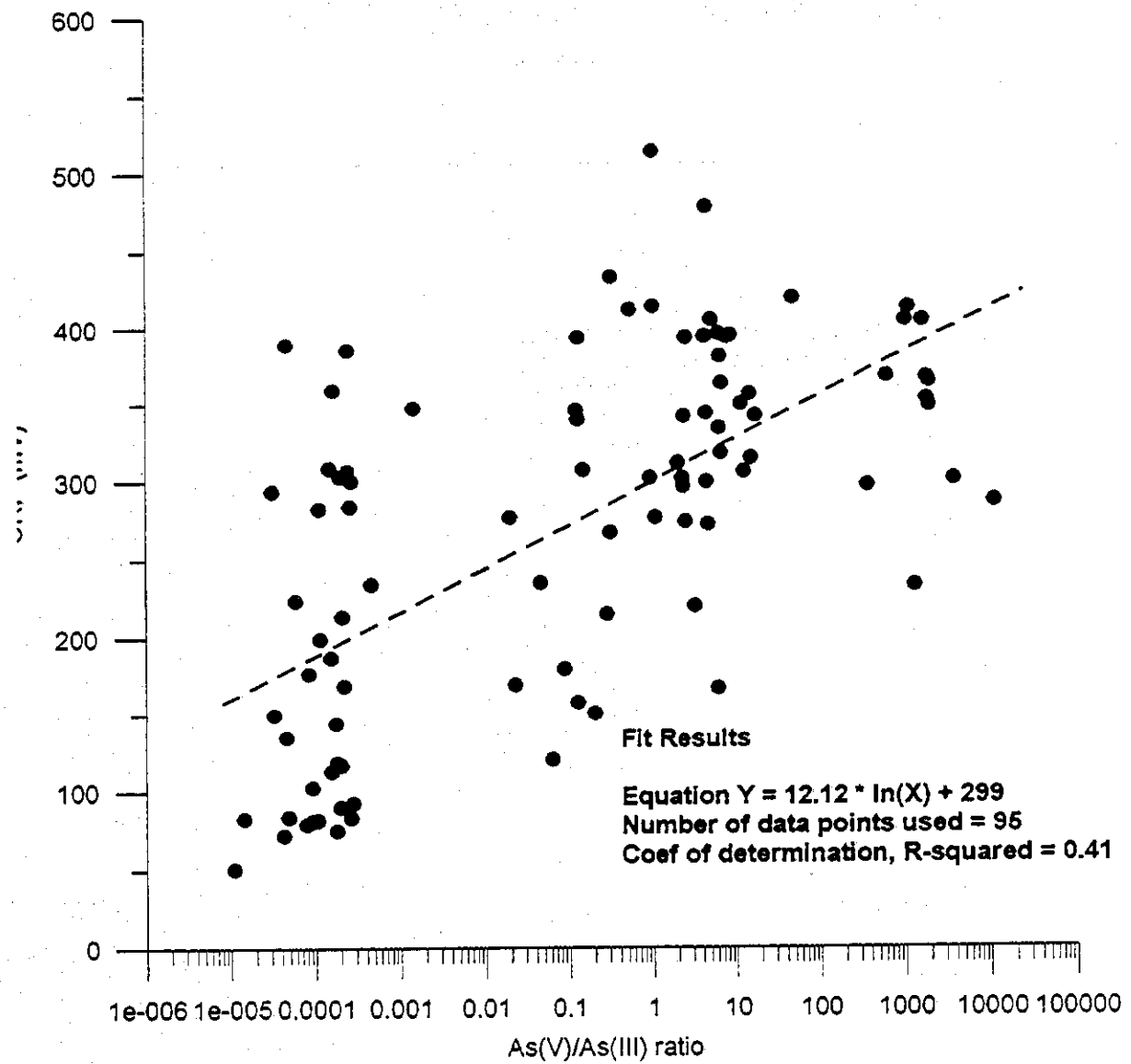

Fig 4.12 As(V)/As(III) Ration and ORP (2)

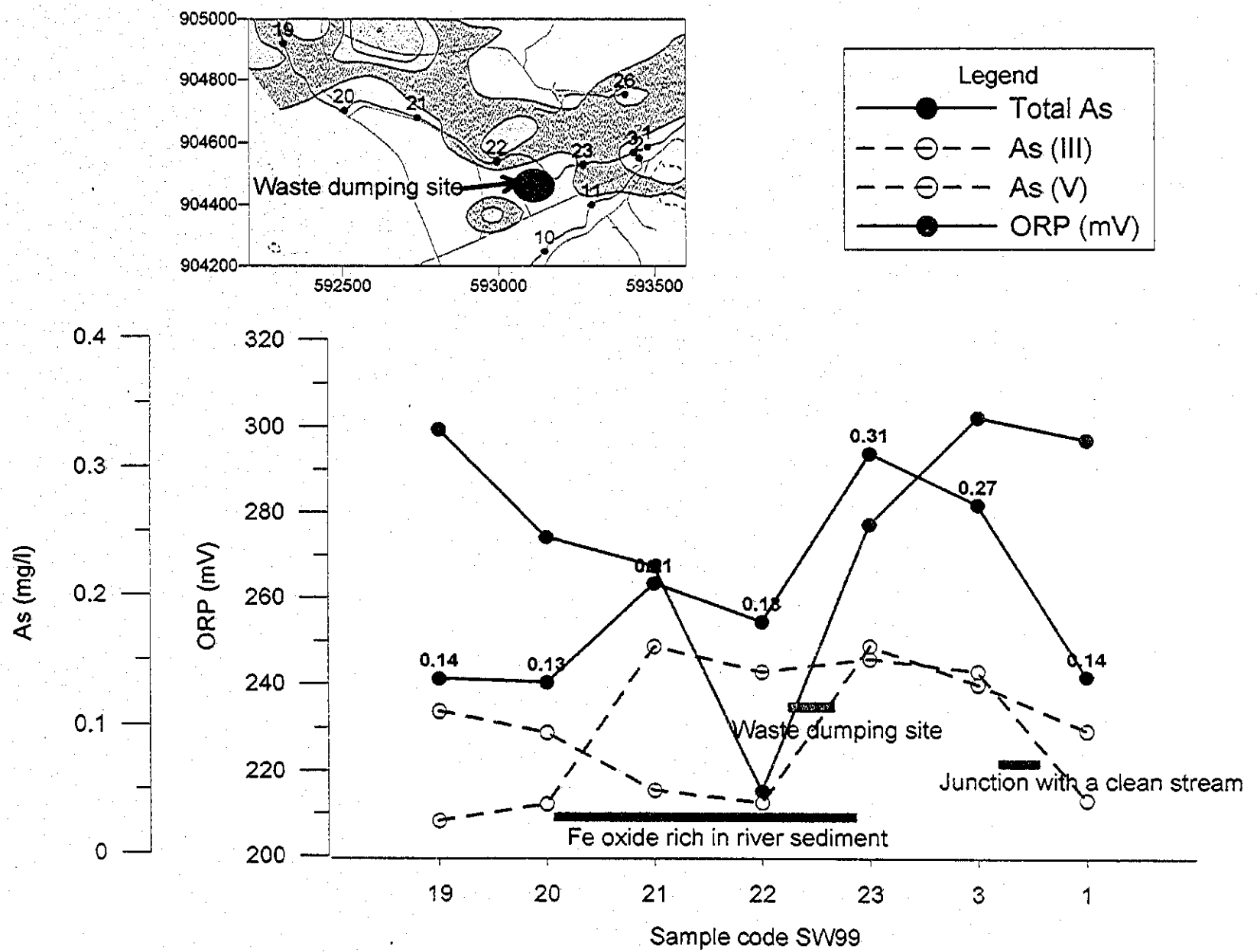

Fig 4.13 Arsenic Species and ORP in Surface Water

finding to understand the behavior of arsenic in the environment.

Fig. 4.13 also shows a sharp increase of total arsenic and As(V) at the interval between the points 22 and 23. Concentration of As(III) is constant. ORP also shows a drastic change to a more oxidizing condition. It is assumed that water high in As(V) flows into the river. There is waste dumpsite (old) at the southern shore of the river. Arsenic may come from there. An auger survey was carried out to confirm this assumption. High arsenic at 1.7 mg/l in the As(V) form in water and 1.8 mg/l in soil elution were detected. This suggests the disposal of concentration waste at the site. The dumping materials were more porous than normal soil. Then it is in a more oxidizing condition and made As(V) dominant.

4.4 Conception model of contaminant source

4.4.1 The foothill concentrator

Concentration waste dumped in underground was visually confirmed by the trench survey. Over 100 mg/kg of arsenic was detected in soil elution test. Sequential extraction of the soils shows highly varying composition among the samples such as high in water-soluble and ion exchangeable phase or high in sulfide phase. It is clear that this waste constitutes an arsenic contamination source. Relatively high arsenic concentration was detected in the soil downstream suggesting transportation of arsenic from the source. The mechanism can be summarized as follows.

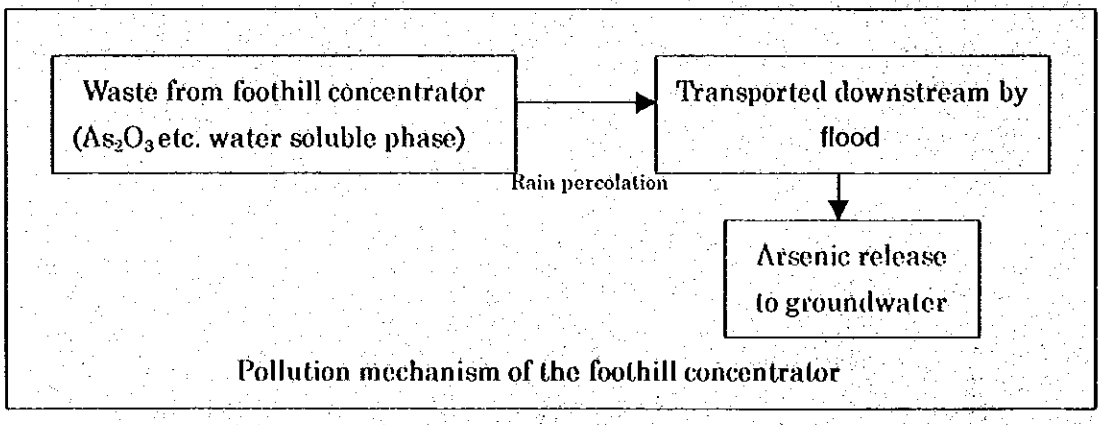

Pollution mechanism of the foothill concentrator

4.4.2 Waste dumpsite (old)

Sample 34 at the waste dumpsite (old) shows high arsenic concentration at 1.8 mg/l by the soil elution test. Also As(V) dominates in the oxidizing condition as discussed before. Therefore it is unlikely that arsenic concentrated on Fe oxide naturally and was released by the reducing condition. It is assumed that concentration wastes from the foothill and the town concentrators were partially dumped to the site. Arsenic was released to groundwater by rain percolation.

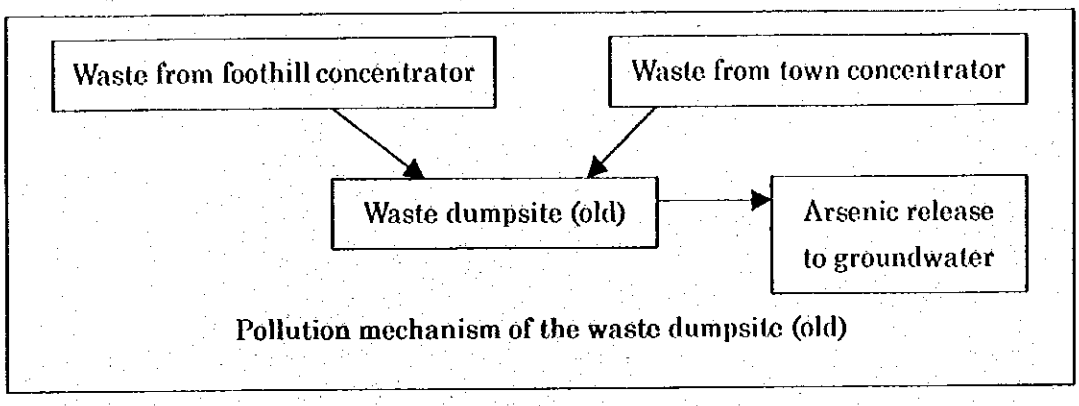

Pollution mechanism of the waste dumpsite (old)

4.4.3 The town concentrator and dredging pond

Fig. 4.14 shows a cross section model around the town concentrator. The location of the cross section line is shown by a dotted line in Fig. 3.16. The arsenic content in auger water is shown as a red line in the figure. It is assumed that arsenic polluted water in the dredging pond is flowing to the town and further downstream. There are points locally low in arsenic. This can be explained by localized groundwater movement and local adsorption of arsenic onto Fe oxide under a reducing condition.

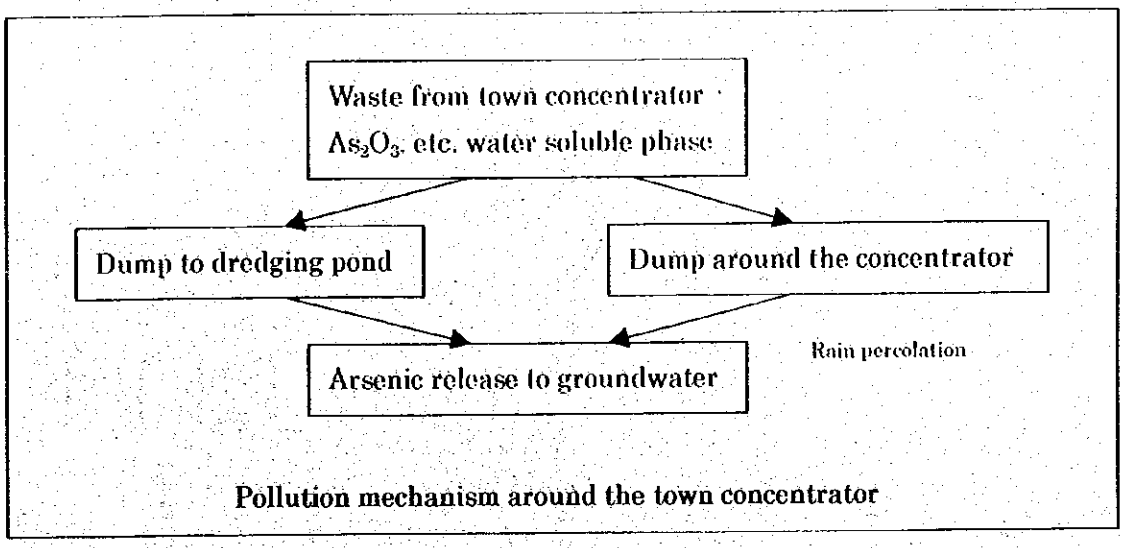

Pollution mechanism around the town concentrator

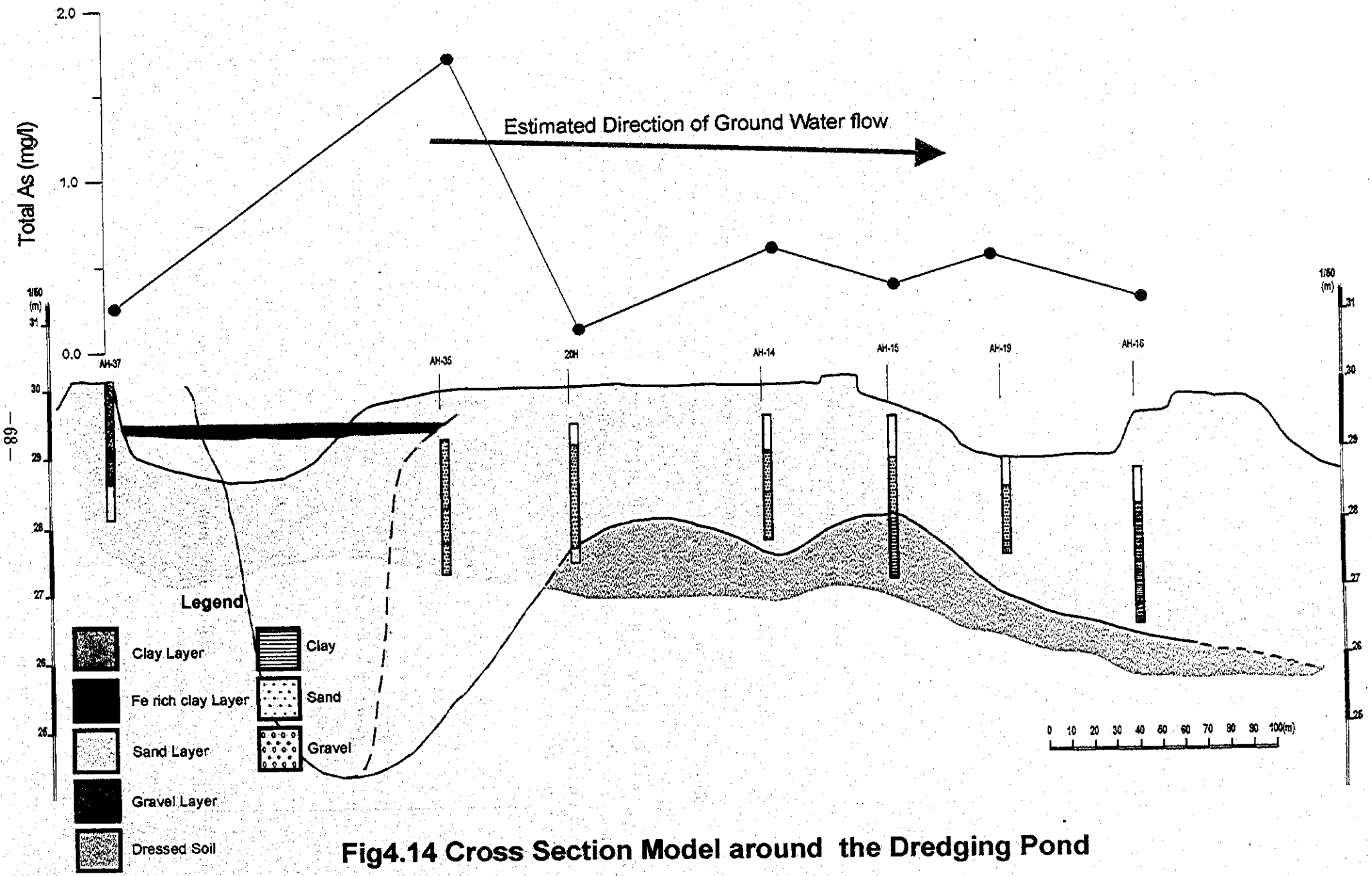

Fig4.14 Cross Section Model around the Dredging Pond

4.4.4 Waste dumpsite (new)

Sample from the waste dumpsite (new) shows high arsenic concentration in auger water, but low arsenic concentration in soil elution test. Considering high concentration of dissolved iron, Fe(II) ion and low ORP at the site, it is assumed that adsorbed arsenic on Fe oxide was released by reducing condition. Sequential extraction result showing high sorbed and organic phase supports the assumption. However, it is risky to conclude that a single mechanism controls pollution and the waste dumpsite may contain some concentration waste.

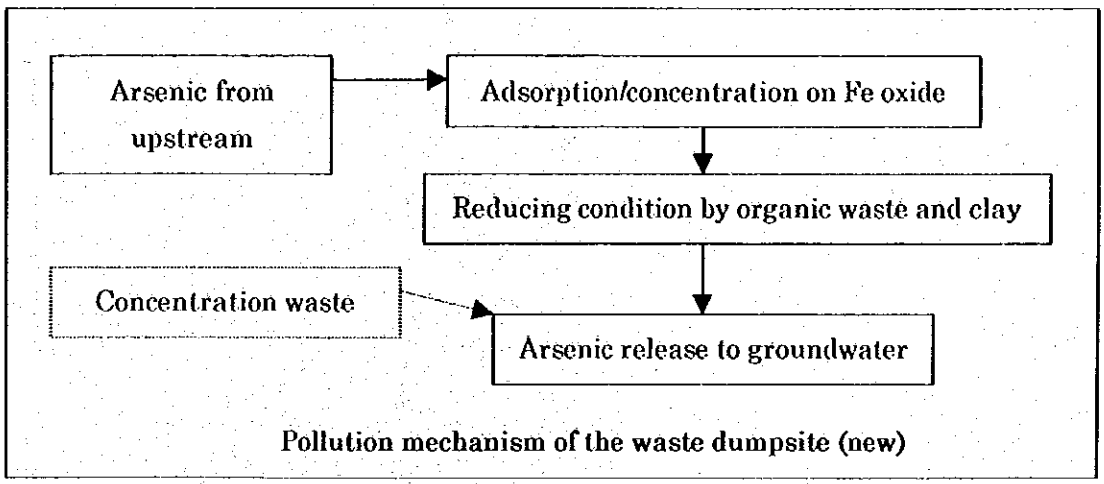

Pollution mechanism of the waste dumpsite (new)

4.4.5 Around site 32C

Fig. 4.15 shows the cross section model around the site 32C. The location of the cross section line is shown by a dotted line in Fig. 3.19. Arsenic and Fe(II) content in auger water as well as ORP are shown by colored lines in the figure. The highest arsenic concentration was observed at the point 32C where ORP becomes reducing by overlying clay. ORP is inversely correlated with arsenic. At the point 22 where it is relatively far from the surface stream, arsenic content decreases though it is high in Fe(II) ions. From these observations, the following model based on arsenic release from Fe oxide by reduction is considered.

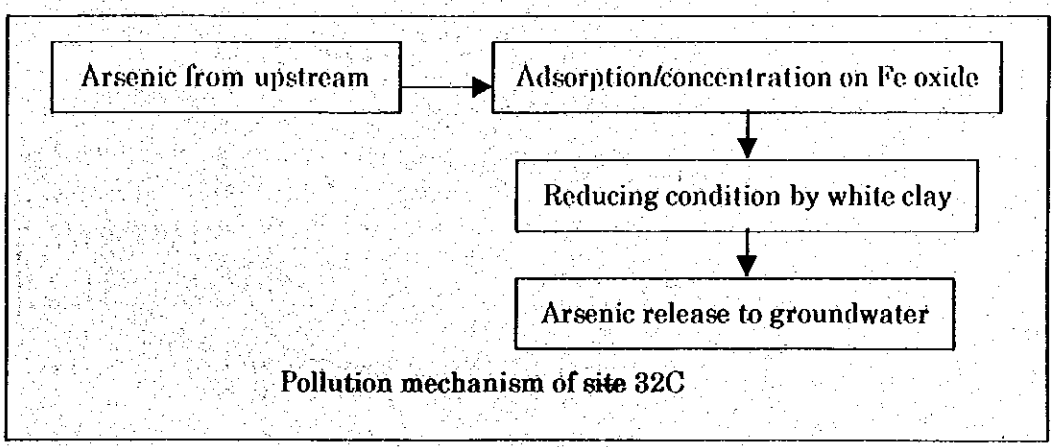

Pollution mechanism of site 32C

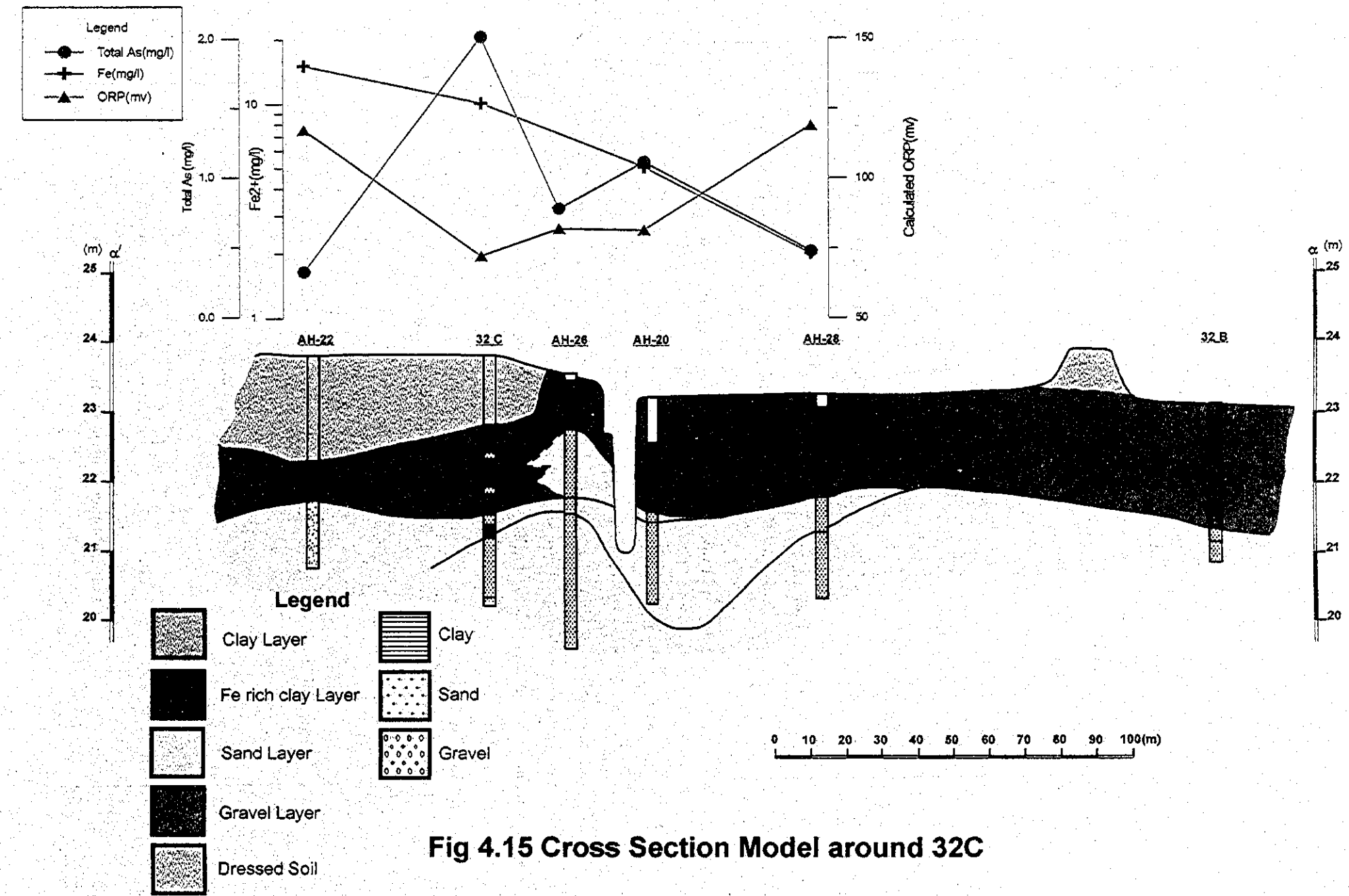

Fig 4.15 Cross Section Model around 32C

Red soil rich in Fe oxide was widely distributed around the shooting range on the north of the site. Arsenic over 1 mg/l is detected at the point 104 in the north. However at the point 42, further upstream, it does not show any arsenic. This may be due to the local ORP condition controlled by a small water pool on the surface.

4.4.6 Around site 32L

Fig. 4.16 shows a cross section model around the site 32L. The location of the cross section line is shown by a dotted line in Fig. 3.21. Arsenic content in auger water is shown by a red line in the figure. It is clear that the dressed soil brought from outside is the contamination source. As shown in Fig. 3.21, arsenic content and ORP does not correlate in general, though there are some spots high in arsenic with low ORP. From the sequential extraction, it was known that the composition of the arsenic phase varied considerably among the soil at the site. It is assumed that mining waste was mixed in the soil brought from outside.

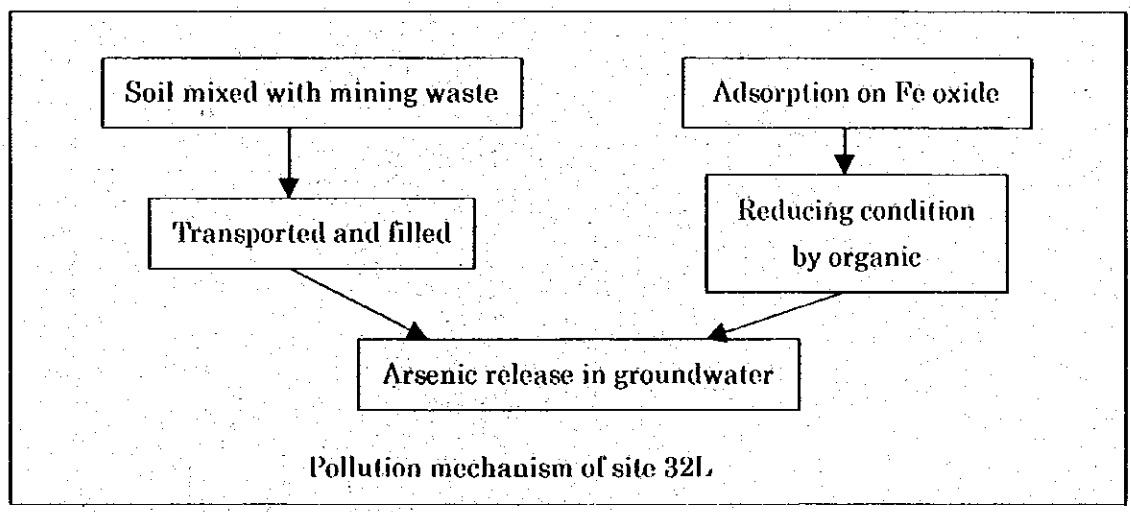

Pollution mechanism of site 32L

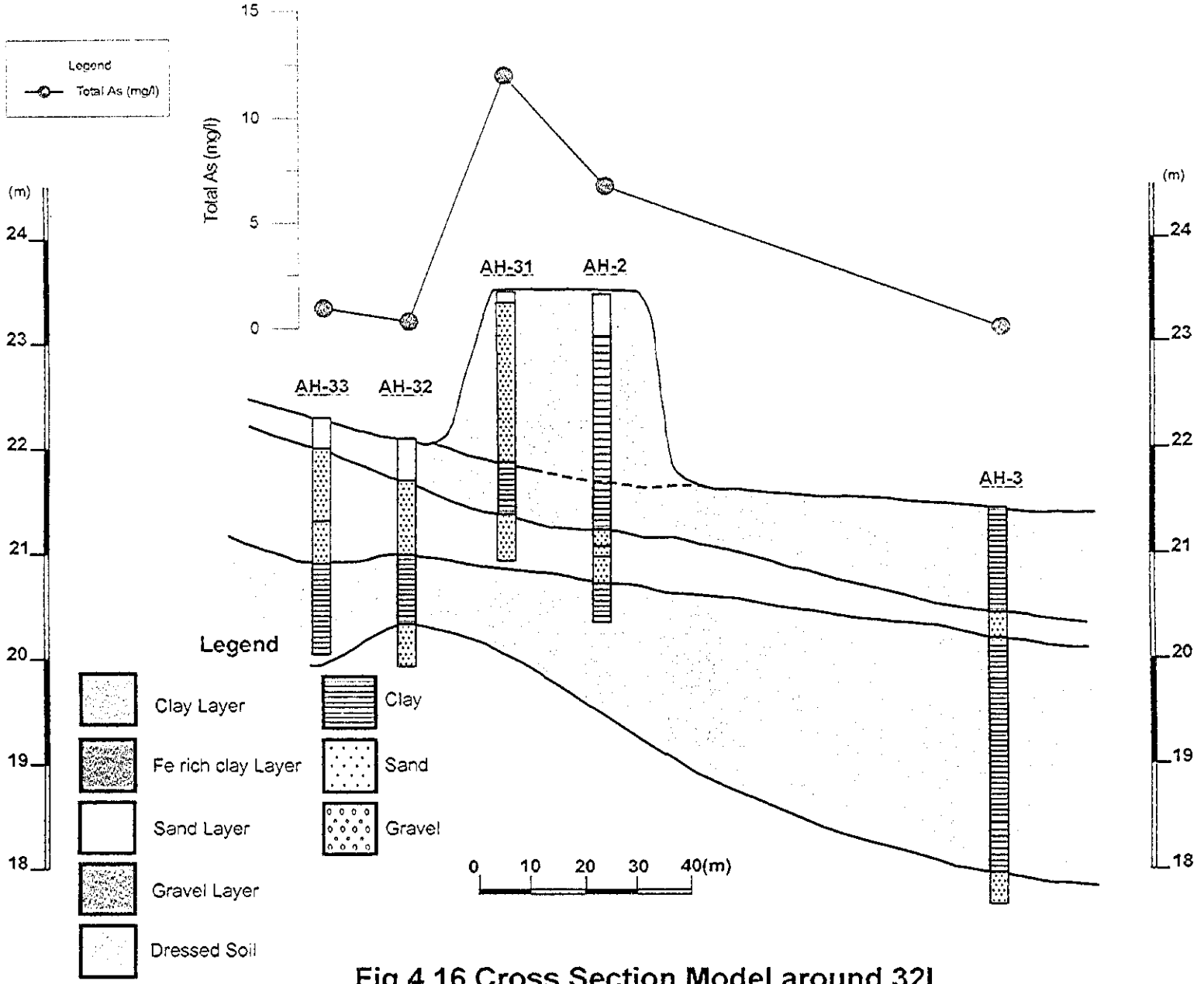

Fig 4.16 Cross Section Model around 32L

5. Study of contaminant transport model

5. Study of contaminant transport model

Fig.5.1 shows the summary of the survey and the resulting maps.

5.1 Groundwater movement

5.1.1 Water mass balance

5.1.1.1 Meteorology

Two meteorological observation stations were established, one representing the mountainous area and the other the plains. An automatic recording instrument was installed at each station during the first field survey in Thailand (October 1998). Five items were observed: temperature, humidity, wind direction and velocity, and precipitation. The locations of the meteorological observation stations are shown in the hydrogeological map (Fig. 5.10). Observations were continuously carried out at 30-minute intervals until June 1999 when the third field survey in Thailand culminated.

Temperature

During the observation period, the average daily temperature fluctuated between 23.4 to 28.9°C, averaging 26.5°C, and gradually dropped from early October, the start of the rainy season, and then rose in late January at the beginning of the dry season.

In contrast, the average temperature in the mountainous area is about 0.6°C lower than the temperature in the plains.

Precipitation

Fig. 5.2 shows the cumulative rainfall in the meteorological observation stations. In spite of being only 3.1 km apart, daily rainfall observations in the two stations showed a huge difference, thereby resulting in a discrepancy of over 300mm in cumulative rainfall. This result indicates that temperature and rainfall in the study area are strongly influenced by local characteristics, e.g. topography.

Humidity

A humidity ranging between 67% to 98%. The survey also shows conditions are more humid in the mountainous area than the plains.

Wind velocity & direction

Data obtained in the latter half of the rainy season in 1998 shows that northern winds prevailed in the area. The northwest winds prevailed at the start of the

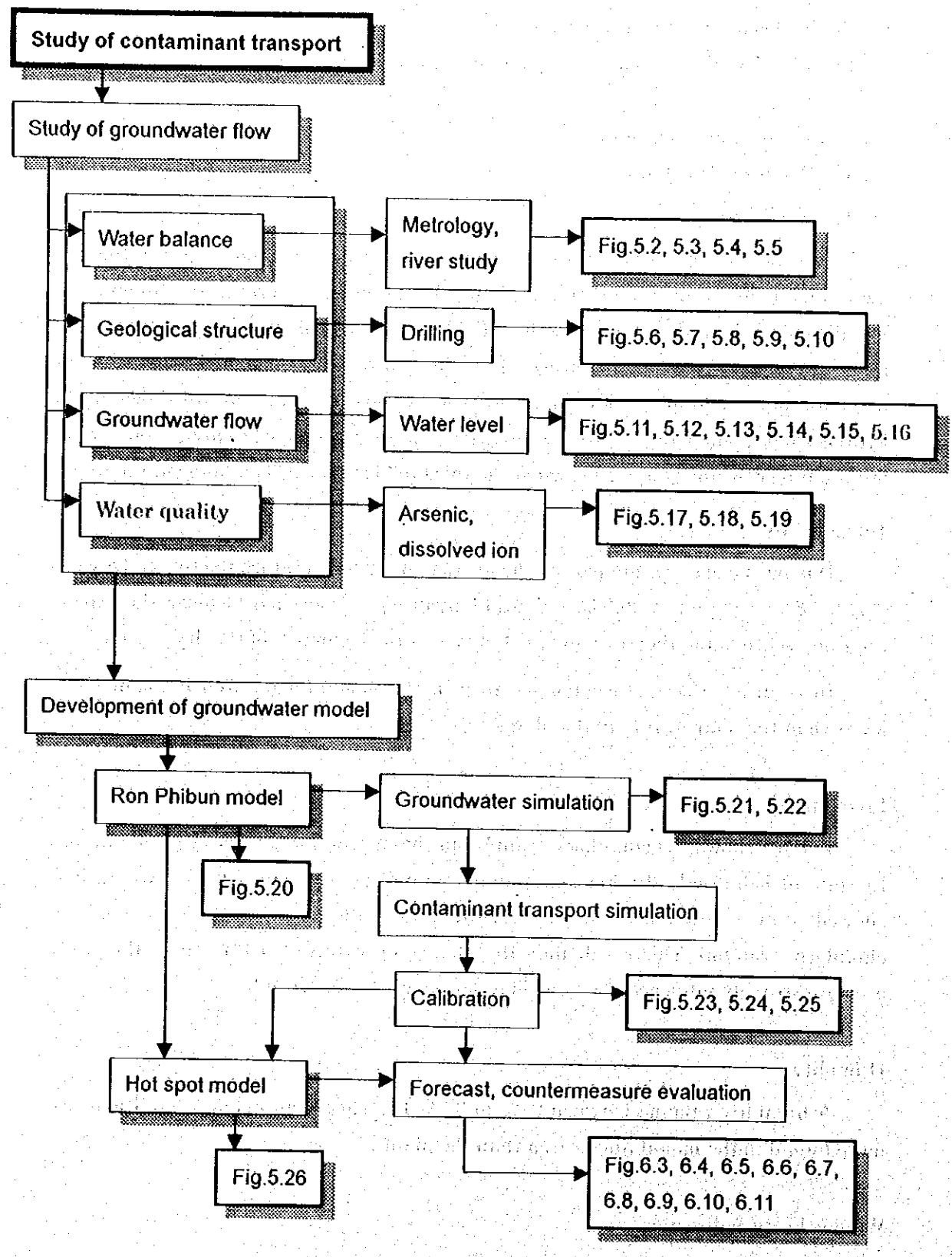

Fig.5.1 Survey Flow of Arsenic Transport Model Study

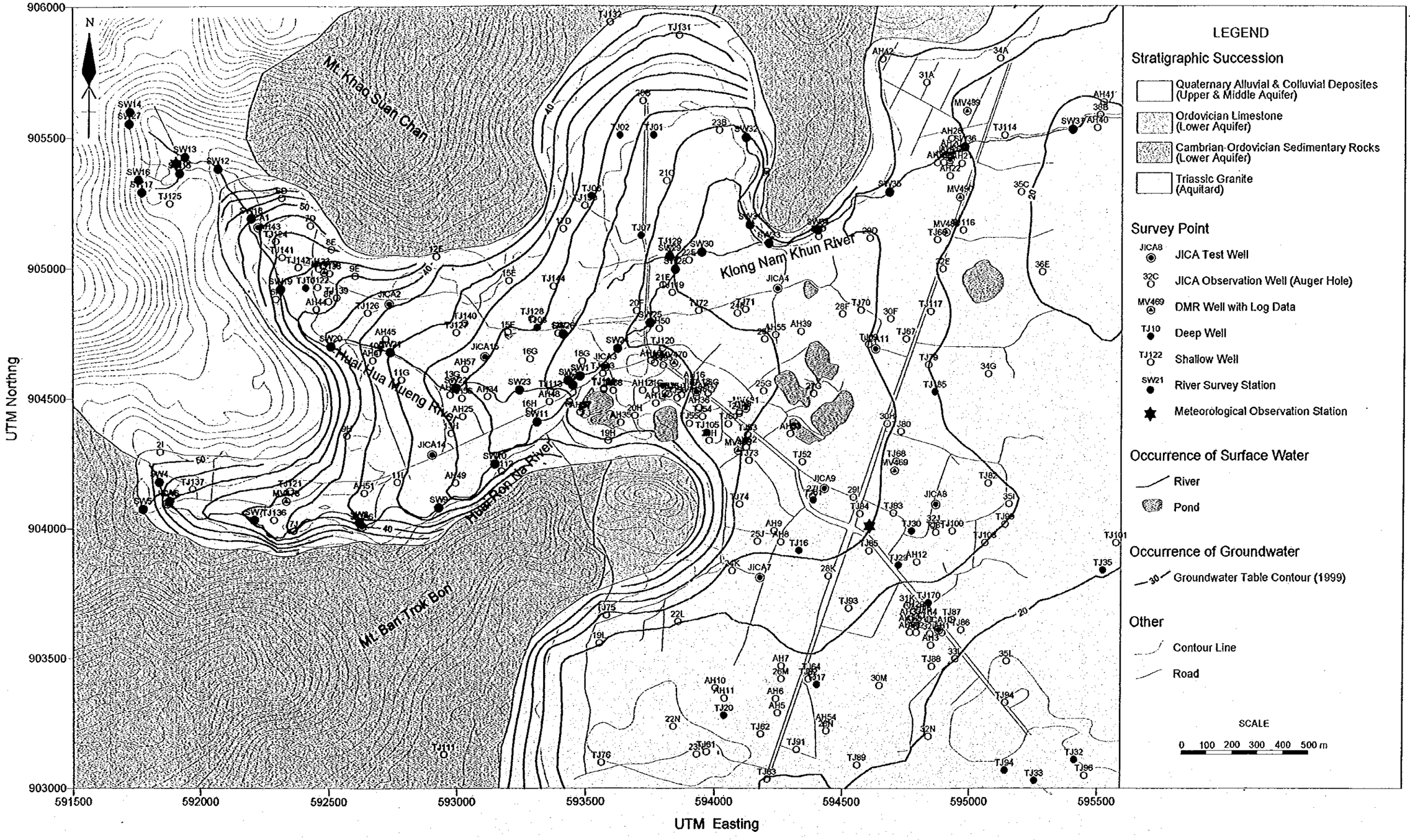

Fig 5.10 Simplified Hydrogeological Map

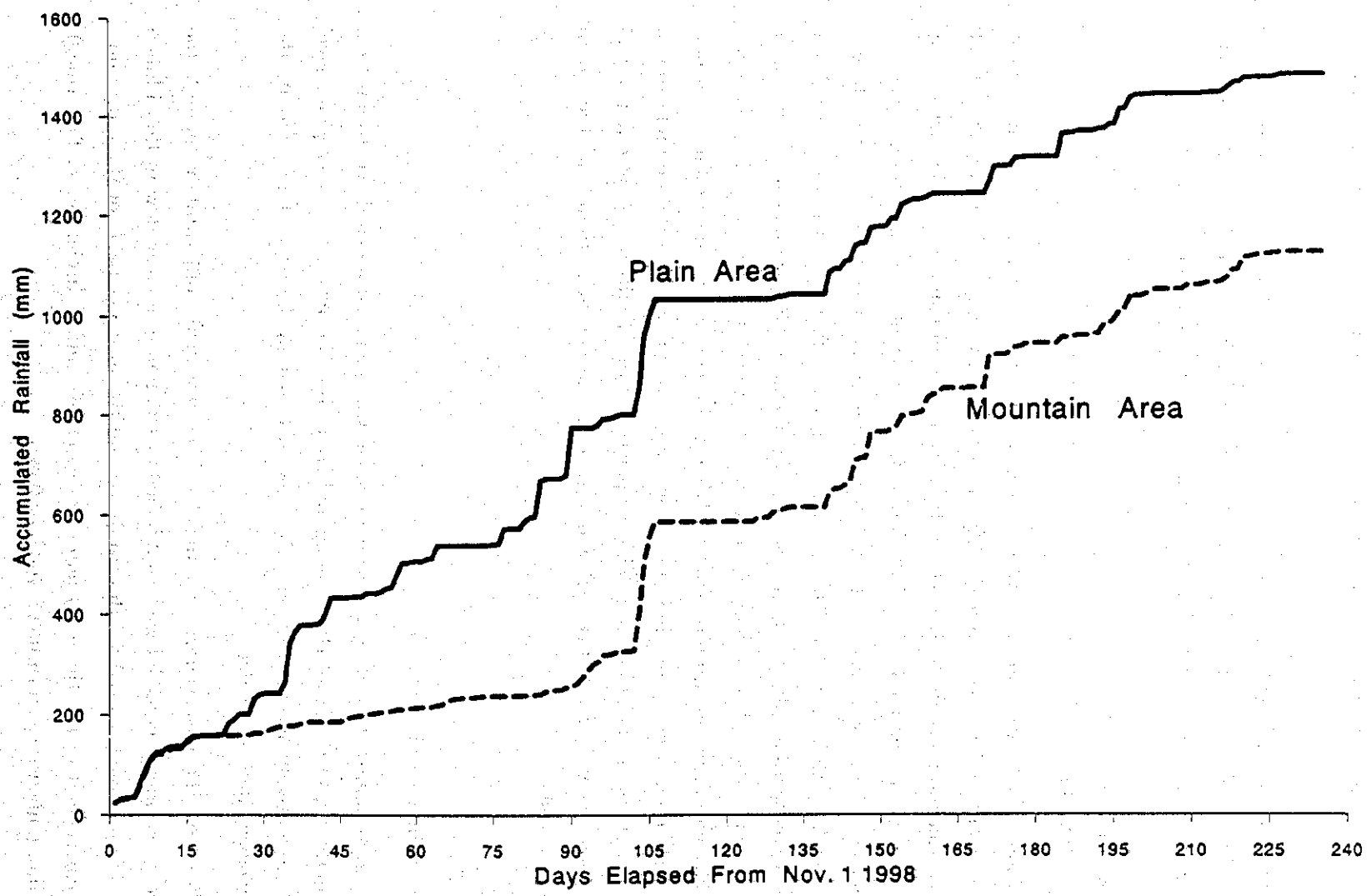

Fig 5.2 Accumulated Rainfall in the Study Area (1998/11/1-1999/6/23)

observation and gradually became northeasterly during the observation period. Except for a slight difference, the wind direction in the plains and mountainous area is congruent.

During the observation period, the average daily wind velocity was from 0.1 to 3.5m/s. Except for December, the average daily wind velocity was less than 2m/s. The average daily wind velocity is slower in the mountainous area than the plains.

5.1.1.2 River Flow

(1) Base flow

More than 40 stations were selected for river survey, including runoff measurement and in-situ water quality observation. River surveys (4 times in total) were carried out twice in the first (1998 dry to rainy season) and third (1999 dry season) field survey in Thailand. Fig. 5.3 shows distribution of survey stations. Fig. 5.4 summarizes the survey results of 1998 dry season. In most stations, the river flow is small at less than 0.1m^3/s. The tendency of river flow to increase toward the downstream section indicates that river water is recharged by groundwater, however, in contrast with the adjacent survey stations, the river flow was found to decrease downstream in several stations. This, together with the results of the groundwater flow survey mentioned hereafter, indicates how river water flows into the groundwater in several sections in the study area. The comparison of the results of the first and second river flow survey shows that river flow in the rainy season is more than twice the flow in the dry season

(2) High-water discharge

An automatic recording water level gauge was installed 300m downstream from the confluence of the Huai Hua Mueng and Huai Ron Na rivers. The river water level was consecutively observed in the rainy season to obtain the basic data to create the hydrological analysis model.

Based on the observed river water level, river runoff, and rainfall amount, the hydrological analysis model was established to simulate the river flow in Ron Phibun basin. Tank model is used for this analysis, and the model consists of three (3) tanks that correspond to the three (3) main processes of rainfall discharge: surface runoff, interflow (subsurface stormflow), and baseflow.

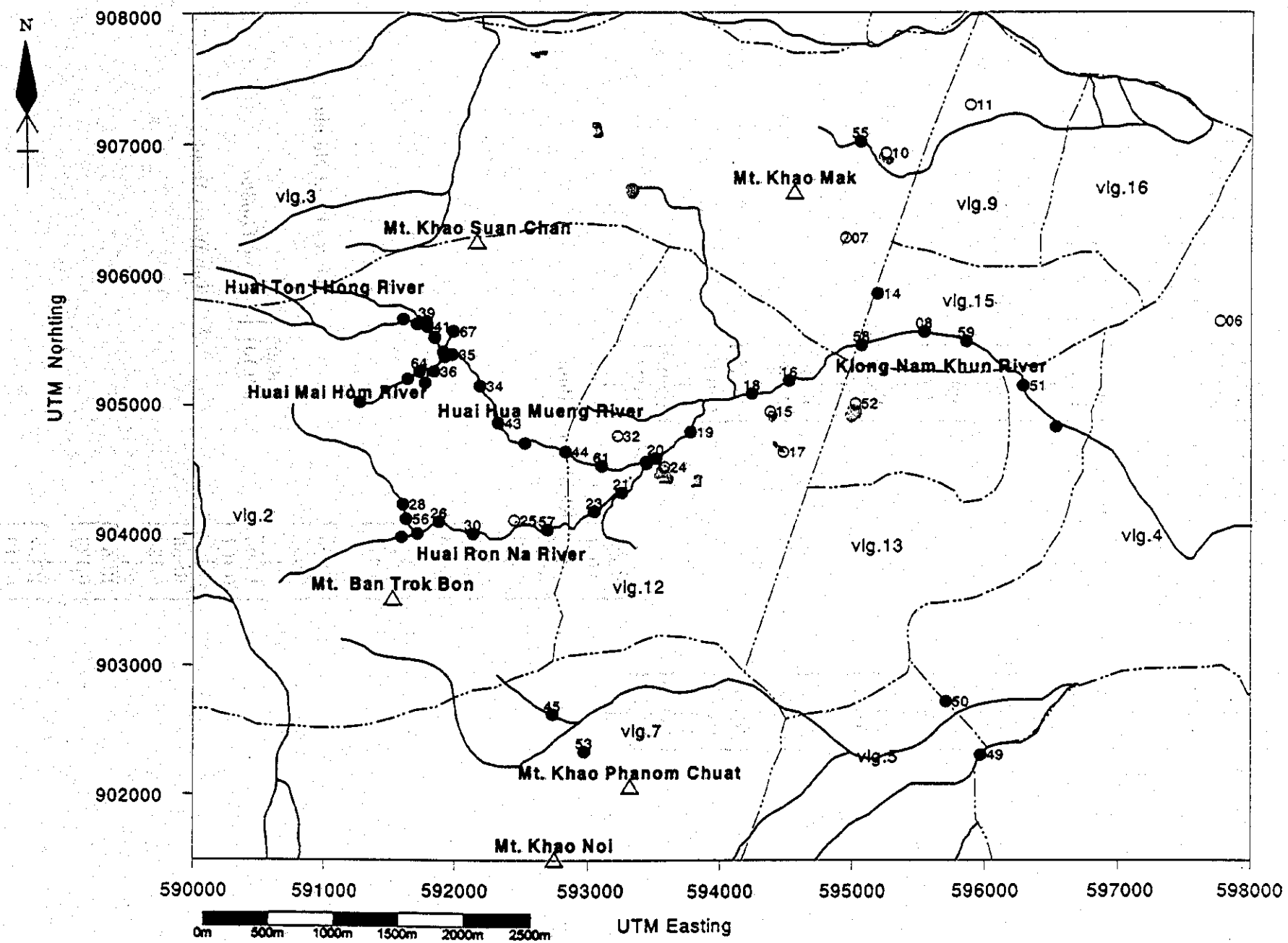

Fig 5.3 Location of Measures Points in the River Survey (Oct. 1998)

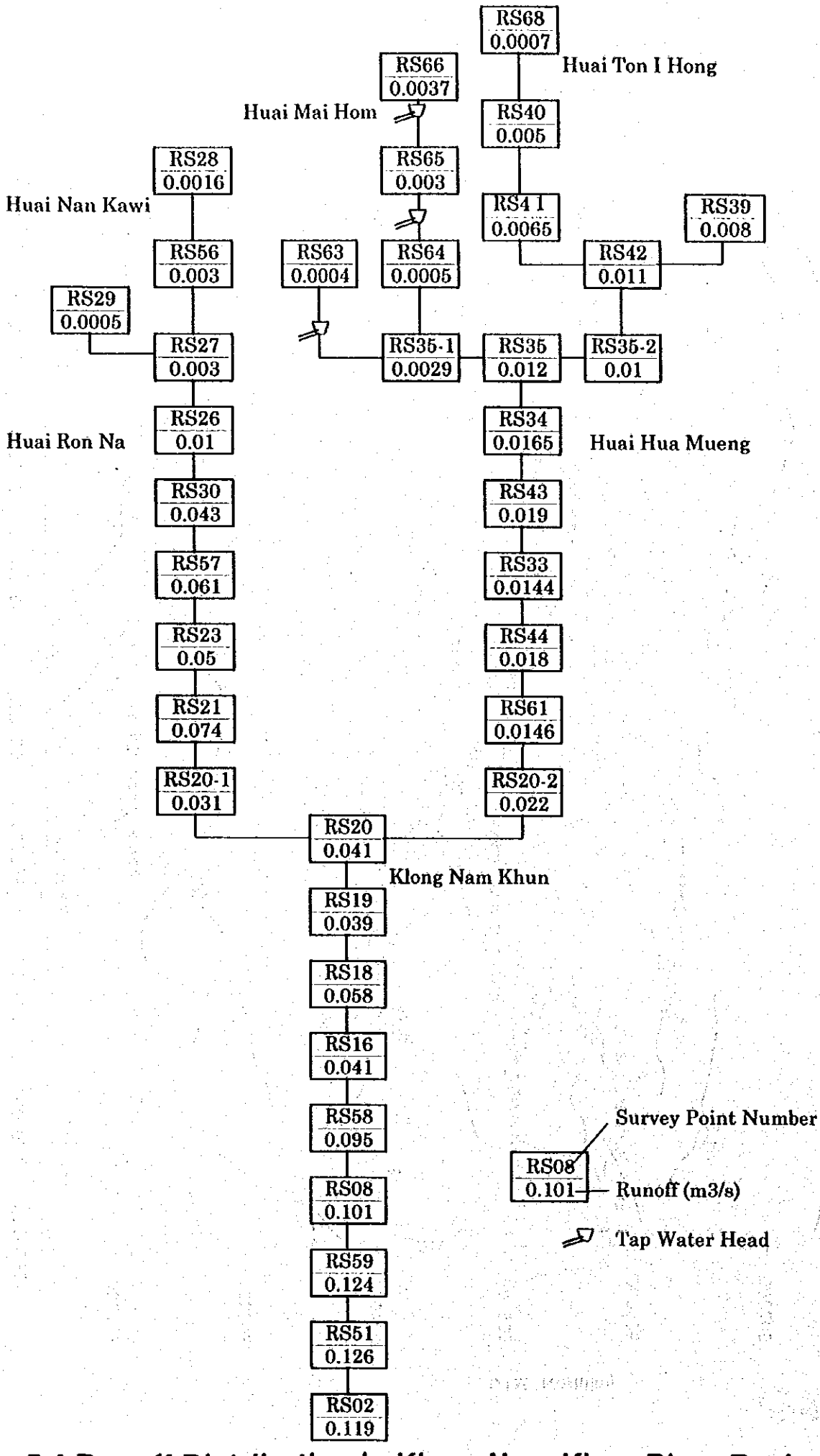

Fig 5.4 Runoff Distribution in Klong Nam Khun River Basin (Oct. 1998)

River flow calculated was verified based on the river flow estimated from the river water level survey results. Fig. 5.5 shows that the calculated value matched the actual value.

5.1.1.3 Water balance in the Ron Phibun basin

The water balance in the Ron Phibun basin was analyzed using data on rainfall obtained from meteorological surveys and the hydrological analysis model. The results are shown in Table 5.1.

Groundwater recharge by rainfall is highest in October; about 60% of the month's rainfall amount. After the rainy season, groundwater recharge declines to a significant degree; negative values were obtained in the months of December and June. This implies a decline in groundwater storage due to the lack of replenishment.

On the other hand, as shown in the table, rainfall in the survey period was higher than in normal years, while the opposite was observed with evapotranspiration. Accordingly, groundwater recharge by rainfall is higher during the study period than in normal years.

Table 5.1 Summary of hydrological analysis using the tank model

	Rainfall (mm)		Evapotranspiration (mm)		Surface Runoff (mm)	Groundwater Recharge	
	Study Year	Normal Year	Study Year	Normal Year		Amount (mm)	Rate (%)
Oct (from 10th)	366	125	33	40	121	212	58
Nov	181	502	44	49	123	14	8
Dec	92	243	44	49	70	-22	-24
Jan	100	50	45	52	51	4	4
Feb	302	45	46	51	197	59	20
Mar	173	87	60	64	69	44	25
Apr	169	129	55	70	71	43	25
May	118	110	56	71	52	10	8
June (until the 23rd)	58	59	39	53	29	-10	-17
Total	1,559	1,350	422	499	783	354	23

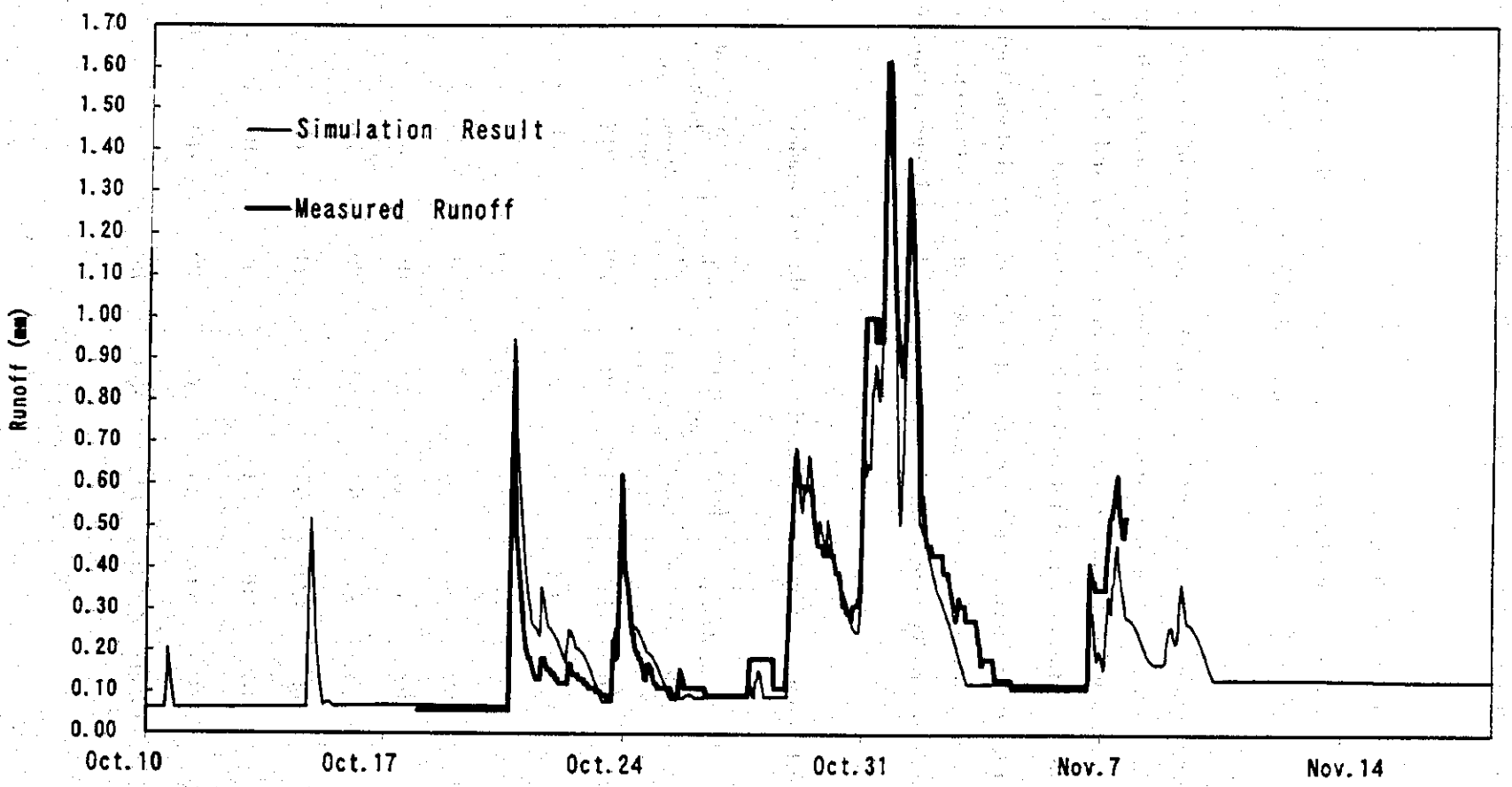

Fig 5.5 Result of Runoff Simulation by Tank Model

5.1.2 Hydrogeological Structure

To understand hydrogeological structure, review of existing data and drilling survey at 15 locations for shallow and deep aquifers including pumping test were conducted. Fig. 5.6 and Table 5.2 summarizes the location and quantity of the drilling survey.

5.1.2.1 Geology

Geologically, Khao Laung Mountain range is made up of Triassic granite, Cambrian-Ordovician shale, siltstone and Ordovician limestone crop-out along the eastern border of the mountain striking approximately NE-SW. The Khao Suan Chan Mountain (318m in elevation) and Khao Mak Mountain (265m in elevation) north of the district, and the Ban Trok Bon Mountain (over 260m in elevation) in the south are mainly made up of sandy shale and limestone.

The basins of the Huai Hua Mueng and Huai Ron Na rivers, the main rivers that pass through the study area, are made up of quaternary colluvial deposits and fluviatile deposits of sand, gravel and clay, from the diluvial to the alluvial periods.

The colluvial slope where Ron Phibun town is situated forms a basin as it is bordered by mountains on the north-south and west sections. The alluvial plain east from the way out of the basin is made up of alluvial layers of sand, gravel and clay.

5.1.2.2 Aquifer group

Based on the records on geological stratum collected in the well inventory survey and the results of the drilling tests, the Ron Phibun groundwater basin within the study area can be divided into 4 hydrogeological units, as shown in Table 5.3.

Table 5.3 Summary of aquifer group

Hydrogeological Units	Geological Periods	Stratum and Lithography	Aquifer
Group 1 Alluvial/Diluvial layers	Alluvial & Diluvial Period	Sand & Gravel	Shallow aquifer
		Clayey soil	Impermeable layer
		Clayey Sand	Deep aquifer
Group 2 Basement rock (Granite)	Triassic	Muscovite-biotite Granite (Weathered Zone)	Aquifer
		Muscovite-biotite Granite (Fresh rock)	Impermeable layer (excluding structure belts)
Group 3 Basement rock (Limestone)	Ordovician	Limestone with fissure and cavities	Aquifer
		Limestone Fresh rock	Impermeable layer

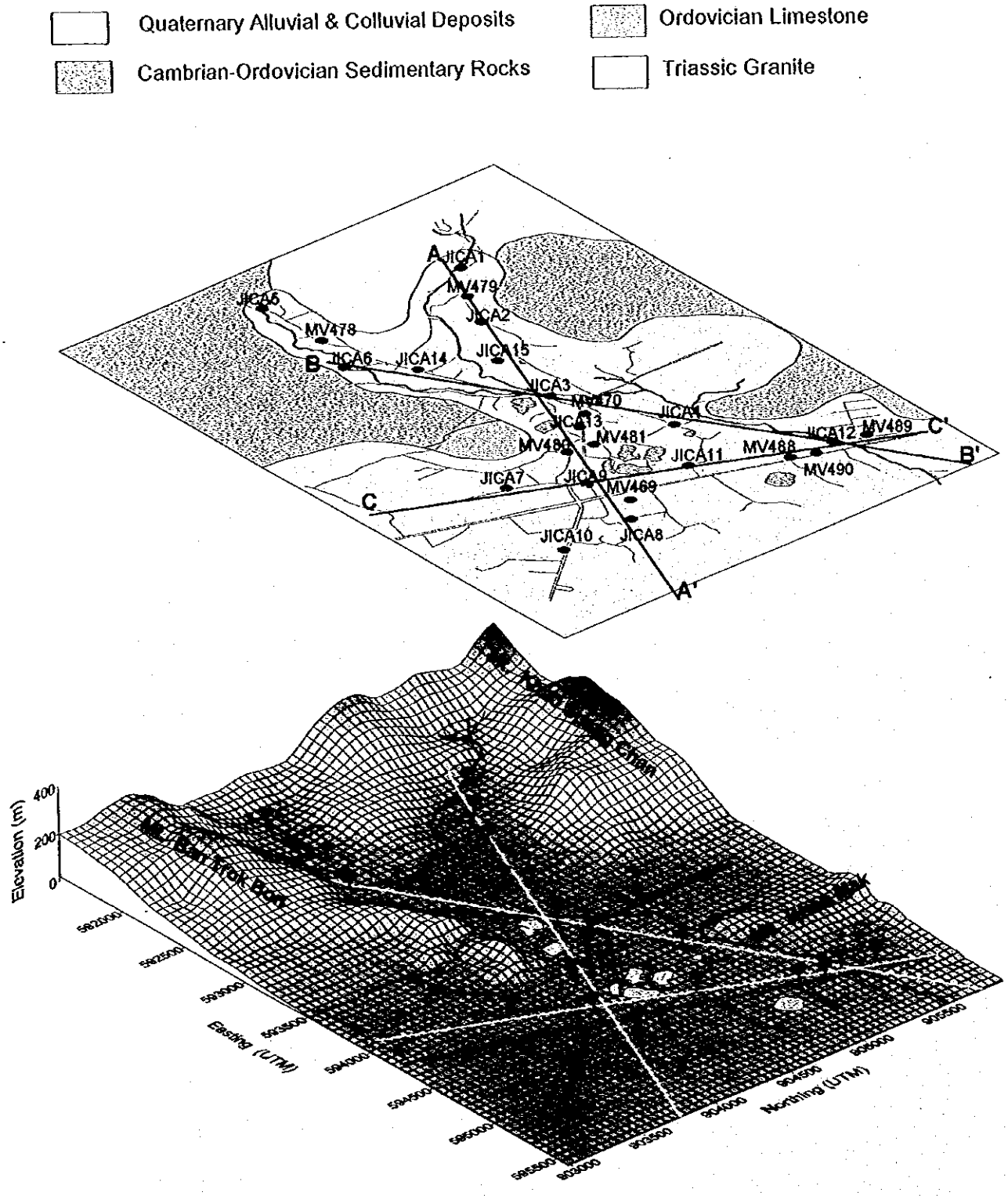

Fig 5.6 Topography and Simplified Geology of Ron Phibun Basin

	No.	Type of Drilling	Drilling Diamter (mm)	Reaming Diamter (mm)	Drilling Depth (m)	3"PVC Instalation		Aquifer	Remarks
						Well Depth (m)	Screen Depth (m)		
Outlined Survey (1st year)	1	Deep Shalow	97.5	150.0	17.00 6.00	14.00 6.00	10.0 ~ 14.0 1.0 ~ 6.0	Deep Shallow	Refilling:14.0 ~ 17.0 m
	2	Deep Shalow	97.5	150.0	32.00 10.00	32.00 10.00	29.0 ~ 32.0 2.0 ~ 10.0	Deep Shallow	
	3	Deep Shalow	97.5	150.0	18.00 9.40	18.00 9.40	7.5 ~ 18.0 1.5 ~ 9.4	Deep Shallow	
	4	Deep Shalow	97.5	150.0	55.00 16.30	66.00 16.30	48.0 ~ 55.0 1.0 ~16.3	Deep Shallow	
	5	Deep Shalow	97.5	150.0	15.60 4.50	15.60 4.50	8.0 ~ 15.6 1.0 ~ 4.5	Deep Shallow	
	6	Deep Shalow	97.5	150.0	21.00 4.00	21.00 4.00	3.0 ~ 21.0 1.0 ~ 4.0	Deep Shallow	
	7	Deep Shalow	97.5	150.0	32.00 4.00	23.00 4.00	10.0 ~ 23.0 1.0 ~ 4.0	Deep Shallow	Refilling:23.0 ~ 32.0 m
	8	Deep Shalow	97.5	150.0	22.00 3.00	22.00 3.00	18.0 ~ 22.0 1.0 ~ 3.0	Deep Shallow	
	9	Deep	97.5	150.0	10.00 -	10.00 -	5.0 ~ 10.0 -	Deep -	
	No.	Type of Drilling	Drilling Diamter (mm)	Reaming Diamter (mm)	Drilling Depth (m)	4"PVC Instalation		Aquifer	Remarks
						Well Depth (m)	Screen Depth (m)		
Detailed Survey (2nd year)	10	Deep 2 Shallow	97.5	150.0	29.00 3.50	27.80 3.50	14.8 ~ 27.8 2.5 ~ 3.5	Base Rock(Limestone) Shallow	Refilling:14.8 ~ 27.8 m,6' CP insert(0~15 m) To prevent from collapsing
	11	Deep 2 Deep Shallow	97.5	150.0	34.50 10.30 7.30	34.50 10.30 7.30	19.5 ~ 34.5 8.4 ~ 10.3 1.0 ~ 7.3	Base Rock(Limestone) Deep Shallow	6' CP insert(0~15 m) ,To prevent from collapsing
	12	Deep 1 Shallow	97.5	150.0	22.00 9.00	22.00 9.00	16.5 ~ 22.0 3.8 ~ 9.0	Base Rock(Limestone) Shallow	
	13	Deep 1 Shallow	97.5	150.0	41.50 9.60	41.50 9.60	35.5 ~ 41.5 1.0 ~ 9.6	Base Rock(Limestone) Shallow	
	14	Deep 1 Shallow	97.5	150.0	18.60 11.50	18.60 11.50	14.0 ~ 18.6 6.0 ~ 11.5	Deep Shallow	Refilling:18.6 ~ 21.0 m
	15	Deep 2 Shallow	97.5	150.0	29.50 10.70	29.50 10.70	13.6 ~ 29.5 2.0 ~ 10.7	Base Rock(Limestone) Shallow	

Table 5.2 Summary of Drilling Survey

Hydrogeological Units	Geological Periods	Stratum and Lithography	Aquifer
Group 4 Basement rock (Sandy mudstone)	Ordovician Cambrian	Shale & siltstone with fissures	Aquifer
		Shale & siltstone (Fresh rock)	Impermeable layer

Fig. 5.7, 5.8 and 5.9. show the distribution of each group along the profile sections.

① Group 1 (Alluvial/diluvial layers)

Shallow aquifer (sand & gravel layer)

The quaternary alluvial layer and colluvial deposits of group 1 are distributed in Ron Phibun basin and the plain on the eastern side. The deposit of this group consists of all kinds of grains including sand, gravel, silt, and clay. Several hundreds of shallow wells within the study area extract groundwater from this layer, making this layer the most exploited shallow aquifer in Ron Phibun basin. Being directly under the ground, the recharge condition of this aquifer is favorable to be recharged not only by the direct infiltration of rainfall, but also from the surrounding mountain area as well.

Table 5.4 shows the hydraulic conductivity derived from the results of the pumping tests carried on the JICA test wells.

Table 5.4 Hydraulic conductivity of shallow aquifers

Well No.	Hydraulic Conductivity (cm/s)	Well Location (Ron Phibun Basin)
1	0.0825	North of upstream section
2	0.106	North of midstream and upstream sections
3	0.0357	Midstream section
4	0.0287	North of midstream and upstream sections
5	0.0578	South of upstream section
6	0.092	South of midstream and upstream section
7	0.0174	South of downstream section
8	0.00819	South of the plains
10	0.0019	South of the plains
11	0.013	Downstream
12	0.00052	North of downstream section
13	0.00067	South of midstream and downstream sections
14	0.0011	South of midstream and upstream sections
15	0.0075	North of midstream and upstream sections

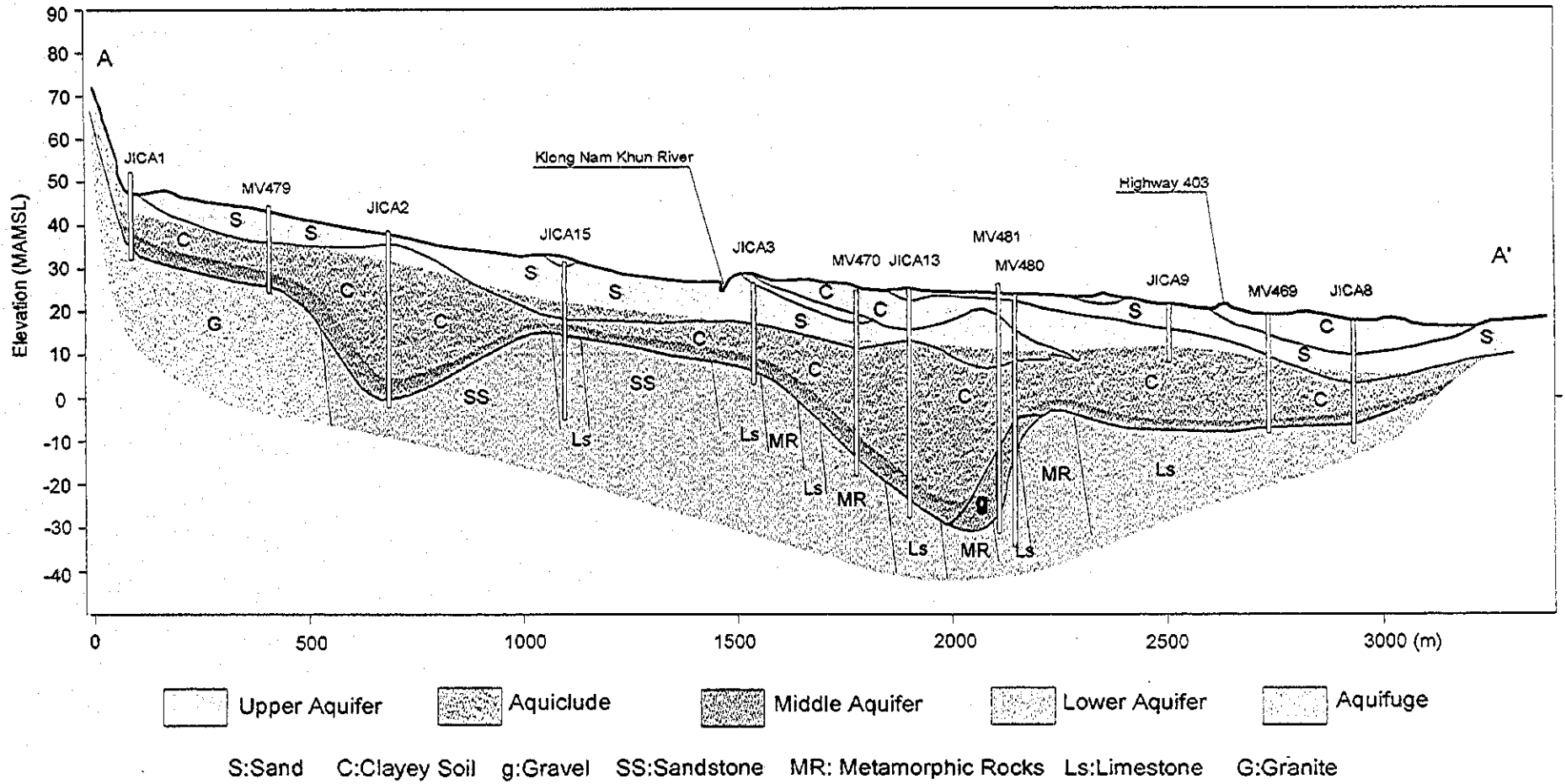

Fig 5.7 Hydrogeological Cross Section A-A'

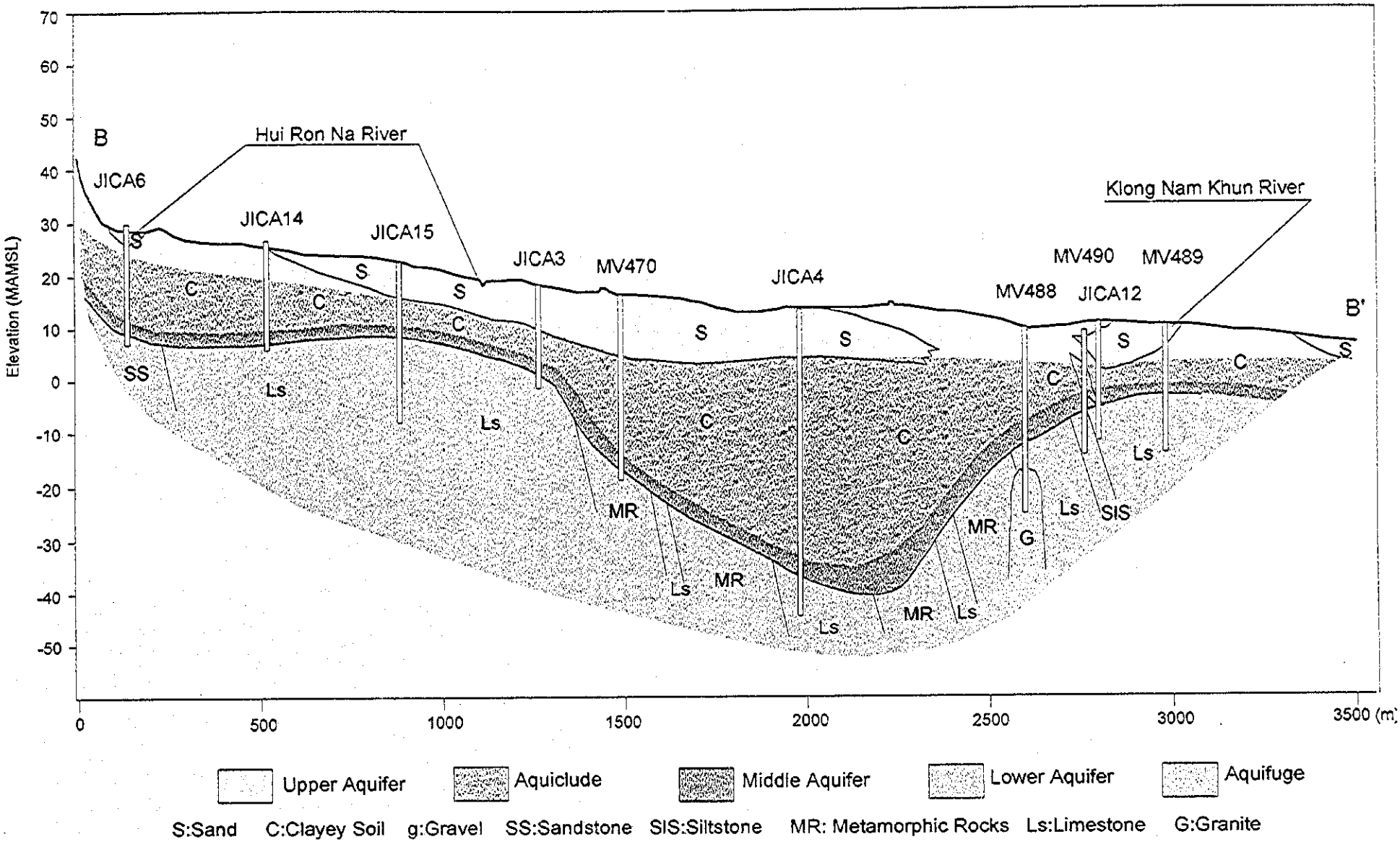

Fig 5.8 Hydrogeological Cross Section B-B'

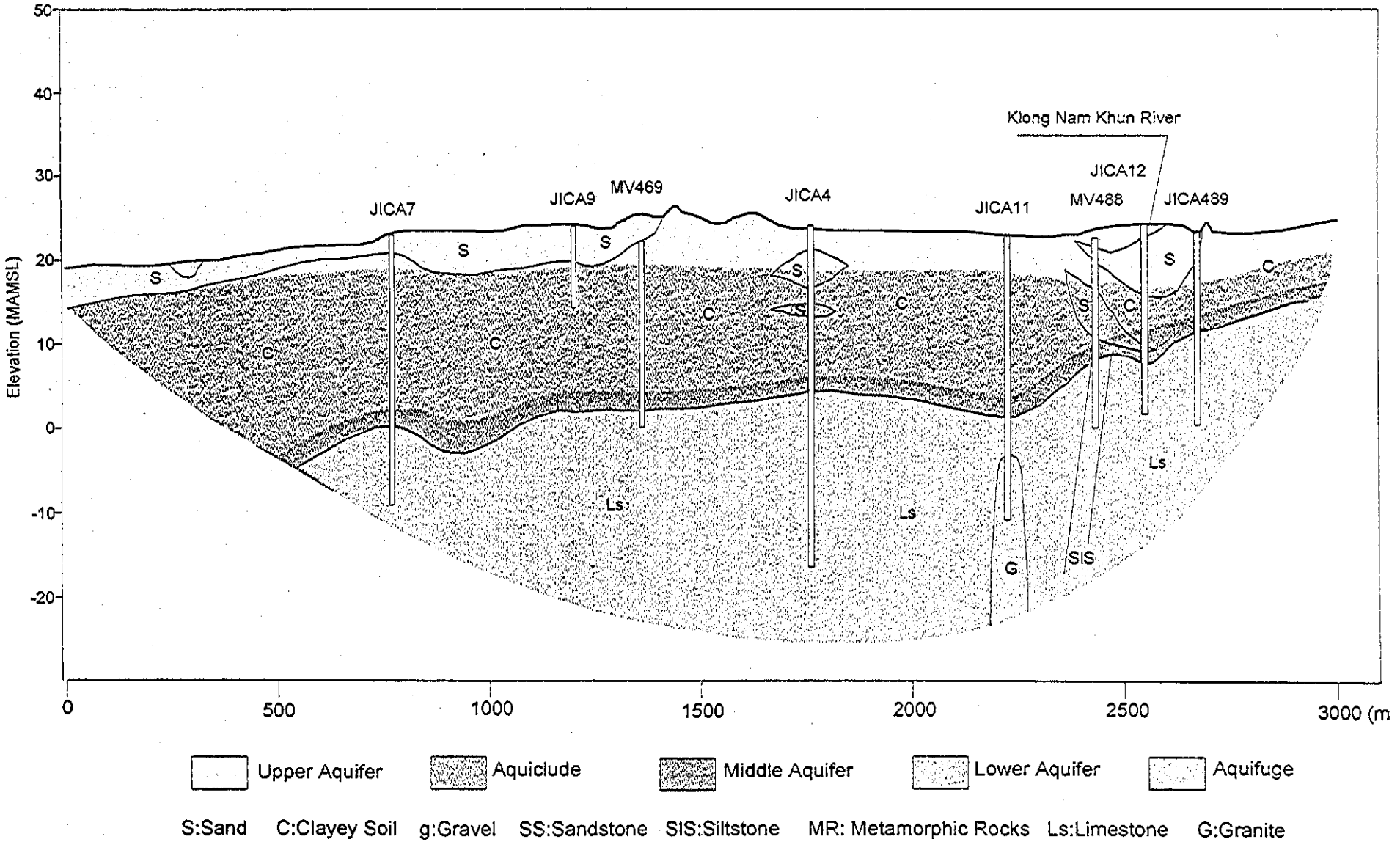

Fig 5.9 Hydrogeological Cross Section C-C'

The hydraulic conductivity of the shallow aquifer varies from 5.2×10^{-3} ~ 1.06×10^{-1} cm/sec, reflecting the change in facies. Overall, the hydraulic conductivity tends to decrease from the upstream section of the basin toward the plain, and from the northern to the southern section.

Impermeable layer (clayey soil layer)

The shallow aquifer directly overlies a clayey soil layer from several meters to over 10 meters thick. The clayey soil layer consists of clay mixed with silt or sand and gravel, or sand and gravel or silt mixed with clay; either composition is high in clay.

Being an impermeable layer between the shallow and deep aquifers, this clayey layer is quite important in the study area. In pumping test, the pumpage of groundwater from a deep well did not affect a water level in a shallow well only several meters away from the test well.

Deep aquifer (sandy soil layer)

The clayey soil layer directly overlies a sandy soil layer from 1 meters to about 20m thick. This layer consists of weathered basement rock and alluvial/diluvial deposits. changing its facies from sand mixed with clay and clay either mixed with sand or gravel. Although the facies seems similar to that of the overlying clayey soil layer, they have quite different characteristics. The layer is looser if the sand and gravel content is high, making core sampling difficult during the drilling test survey. In case it contains more clay. the soil is hard, forming massive structures and a lot of fissures.

This layer directly overlies the basement rock. and as a sandy soil layer aquifer. groundwater extraction through well drilling is possible. Summarizing the results of the pumping test. the hydraulic conductivity of this layer varies from 10^{-2}~10^{-1} cm/s. 10^{-3} on average, and storativity varies from 10^{-1}~10^{-3}, 10^{-2} on average. The specific capacity varies from 10 to 50 l/min/m, 24.6 l/min/m on average. It can be inferred that this layer is not inferior to the other aquifers at least in terms of permeability and the capability to provide water.

As shown in cross-section (Fig. 5.5 to 5.7), this layer is directly in contact with the other aquifer groups and acts as a conduit between the basement rock aquifers.

② Group 2 (Triassic granite)

The granite that makes up the mountain at the westernmost section of Ron Phibun basin forms the backbone of mountain ranges in the southern region of Thailand, including the Ron Na - Suan Chan area.

According to the core samples extracted in the drilling test survey, the granite is deep gray, fine to medium grain muscovite-biotite granite. The granite that makes up the mountain is generally considered as an impermeable basement rock, with the exclusion of the fault belts that contain a lot of fissures..

③ Group 3 (Ordovician limestone)

Limestone layer of group 3 crops out in both sides of the exit of the Ron Phibun basin. The limestone is dark gray in color and forms either a massive or a stratiform structure. Numerous fossils, including corals and crinoid stems were detected in core samples. From these core samples, the limestone was found to tilt at about 45°, corresponding to the results of previous surveys on surface outcrops (45° southeast).

The groundwater amount that can be extracted from the limestone aquifer significantly varies depending on development of fissures and cavities. Core samples show that the limestone has undergone minor metamorphosis, and is relatively rich in fissures. The fissures vary by depth and section, having intervals of 10-30cm. The core samples can only be, therefore, extracted as short columns. A part of the fissures are found to be filled with clay, indicating its role as a groundwater conduit. This aquifer is predominantly exploited as 70% of the deep wells.

④ Group 4 (Ordovician & cambrian sedimentary layer)

Eastern of granite of group 2 distributes the sedimentary rocks of group 4. Fig. 5.7 and 5.8. the geological profile A-A' and B-B', reveals the distribution of layers along the direction of major axis of Ron Phibun basin. Group 4 aquifers in the central basin area are overlain by alluvial and diluvial layers. thereby producing no outcropping sections. However, as shown in Fig. 5.6. outcrops can be seen in the northern part of the Huai Hua Mueng river and the southern part of the Huai Ron Na river, forming the mountains on both sides of the Ron Phibun basin.

According to the core samples of JICA test wells. this group is mainly made up of siliceous sandstone. mudstone and siltstone. however. the core samples taken from the JICA 14 and 15 test wells indicate the presence of limestone. The high temperature and high pressure during the intrusion of granite resulted in a slight metamorphosis, whereby some parts became phyllites. The sandstone in this group is hard and with

well-developed fissures in some sections.

About 10% of the deep wells in the study area exploit groundwater resources in this group.

5.1.3 Groundwater flow & water quality

5.1.3.1 Groundwater level

Simultaneous groundwater leveling was carried out to understand distribution of groundwater level and groundwater flow conditions. Groundwater leveling is shown in Fig. 5.11. Groundwater level in shallow aquifer wells is affected by topographic conditions. In the sections of Huai Hua Mueng and Huai Ron Na river basins, groundwater level fluctuates sharply where the slope is steep. At the vicinity of the shallow aquifer to the basement rock area, the hydraulic gradient is high (more than 1/100). Towards the center of the basin the gradient gradually decreases to about 1/100. As the topography flattens out in the plains, the gradient decreases from less than 1% to about 1/1000.

The direction of the groundwater flow is determined from the groundwater level contour and indicated using a blue arrow. Groundwater flows from the surrounding mountain areas to the central part of the basin in the upstream and midstream sections. Within Ron Phibun basin, groundwater mainly flows from the western to the eastern sections. In the plains, groundwater mainly flows eastward, but changes in micro-topography and localized water use conditions disperse the flow into different directions.

The direction of groundwater flow can be determined only according to the hydraulic gradient, while velocity is the product of the hydraulic gradient and the hydraulic conductivity based on Darcy's law. To determine the groundwater flow velocity distribution within the Ron Phibun basin, a simulation model was established based on the aquifer coefficient and other parameters obtained from surveys of this project. The distribution of groundwater flow velocity is shown in Fig. 5.12.

In the northern upstream section of the basin, both the hydraulic conductivity and gradient are high: groundwater flow velocity is several 10cm/day, over 150m/year. In contrast, the hydraulic gradient and conductivity in the plains are low: the velocity is only several cm/day, less than 10m/year.

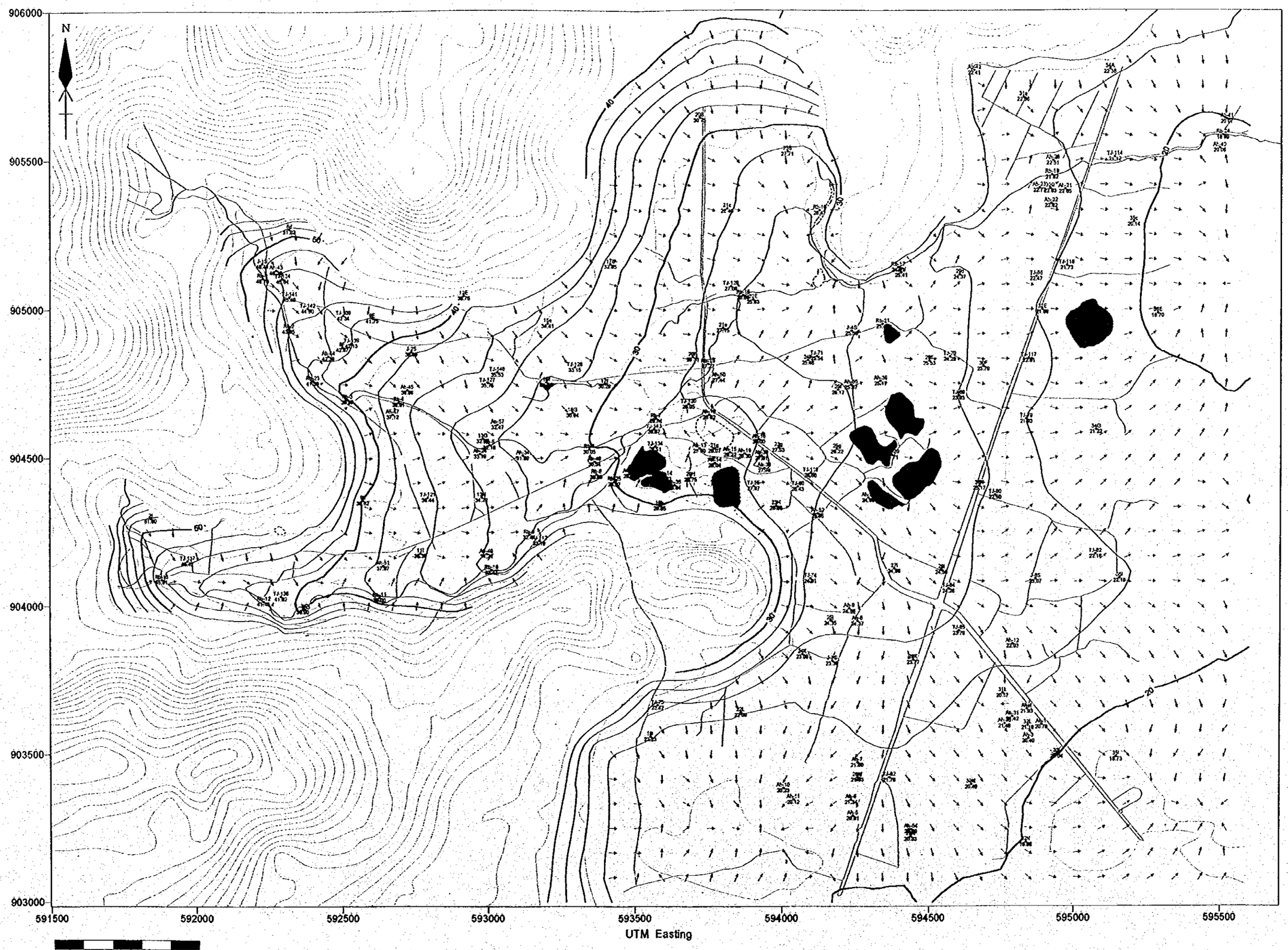

Fig 5.11 Groundwater Level Contour on 21 June 1999

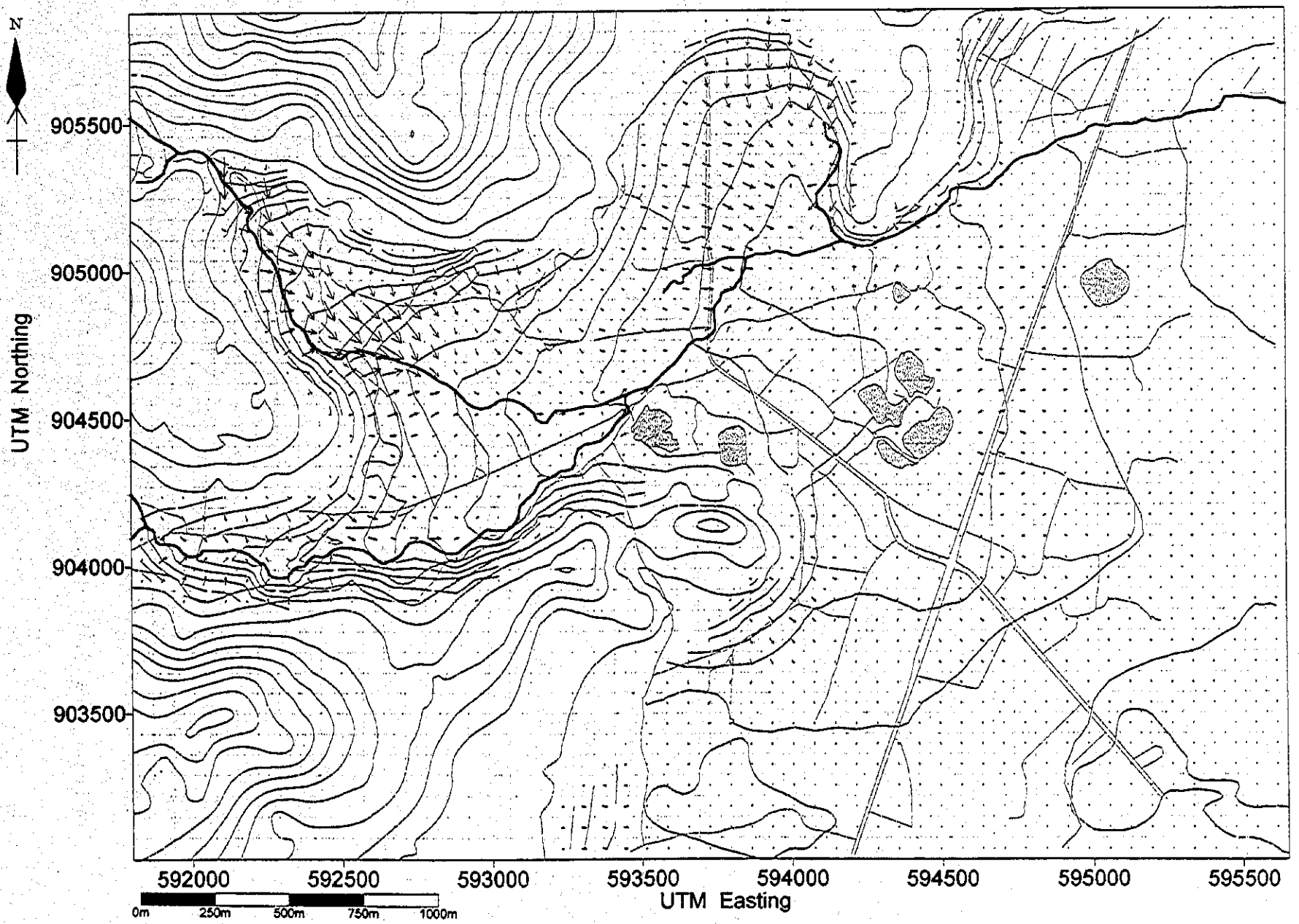

Fig 5.12 Groundwater Flow Velocity in Shallow Aquifer